1-1-1995

Development of a biodegradable nerve regeneration cuff

Ivan Luis Diaz
Iowa State University

Development of a biodegradable nerve regeneration cuff

by

Ivan Luis Diaz

A Thesis Submitted to the

Graduate Faculty in Partial Fulfillment of the

Requirements for the Degree of

MASTER OF SCIENCE

Interdepartmental Program: Biomedical Engineering
Major: Biomedical Engineering

Iowa State University
Ames, Iowa

1995

TABLE OF CONTENTS

LIST OF TABLES

LIST OF FIGURES

1. INTRODUCTION

1.1 General

A peripheral nerve is composed of axons, connective tissues, and non-cellular elements. Nerve injuries can be classified in three categories according to the severity of the lesion: neuropraxia, axonotmesis and neurotmesis. In neuropraxia, there is a localized and temporary (days or weeks) interruption of the nerve conduction at the site of the lesion without loss of nerve conduction or degeneration proximal and distal to the lesion. Normally, the function of the injured nerve is entirely restored. In axonotmesis, there is a separation of the nerve fibers into proximal and distal parts. However, the continuity of the connective-tissue framework and endoneurial tube is maintained. Loss of nerve conduction and degeneration take place distal to the lesion. The time that is needed to recover from this lesion depends on the distance between the lesion site and the muscle to be reinnervated. In the more severe case of neurotmesis, the peripheral nerve is completely severed at the lesion site. Therefore, the nerve function recovery in neurotmesis is poorer than in axonotmesis because the regenerating axons in neurotmesis become easily misguided and fail to

reach their target organs due to the lack of initial connective-tissue framework and endoneurial tubes (Spencer, 1977).

The end-to-end anastomosis is the preferred method of nerve repair to be used on a transected nerve with a gap length less than 10 mm. In case of nerve gaps of 10 mm to 50 mm, a nerve bridge technique is then the preferred method of nerve repair (Rosen et al., 1989). Published information on the use of nerve bridge techniques indicates that regenerated nerves can bridge these gaps (Dellon and Mackinnon, 1988). Nerve bridge techniques include nerve autografts, autologous vein grafts, and artificial nerve grafts. In artificial nerve grafts, the material can be biocompatible and permanent (one example is silicone rubber), or biodegradable (two examples are polylactic acid and polyglycolic acid).

1.2 Statement of the problem

At the present time, the nerve autograft technique is mainly used when a nerve gap is greater than 10 millimeters. The problems with autografts are that another nerve has to be sacrificed and there is increased risk due to a second surgery site. To approach these problems with the nerve autografts, some researchers have successfully used biocompatible artificial nerve grafts (single lumen cuff (SLC) with smooth walls, biodegradable and non-biodegradable) in the repair of transected nerves (Williams et al., 1983; Seckel et al., 1984).

However, the resultant regenerated nerve (using these SLC) had a central or mid-portion narrowing (central tapering). This narrowing could be due to the lack of mechanical support for the regenerating axons in the center of the gap. Also, the single lumen configuration permits the mixing of the different connective tissue layers (intra-neurals and extra-neurals) causing invasion of fibroblasts from the epineurial layer that can interfere with the re-establishment of the perineurial layer and an orderly axonal regeneration. In addition, the non-biodegradable SLC grafts have the problem of remaining in the body as foreign material after the nerve has regenerated, or if removed, the removal of these grafts could cause injury to the healed nerve.

1.3 Approach to the problem

To address some of the problems of nerve autografting, central tapering, the lack of mechanical support at the middle of the gap, mixing of the different connective tissue layers and their poor orientation, and the lack of biodegradability, the present work was conducted. The biodegradable (polylactic acid, PLA) seven-lumen cuff proposed increases the surface area available for cell attachment, provides mechanical support, and offers improvement in orientation and guidance of the regenerating axons (Daniel, 1991). In addition, since the main component of this system is PLA, it offers the advantage of good biocom-

patibility and gradual disappearance with time, generating metabolic products that are used directly by the animal or human body.

However, some of the potential problems of this proposed system (PLA seven-lumen cuff) can be mechanical instability due to their proven biodegradability. One of these problems may be the swelling of the nerve guides, due to absorption of water, that may reduce the luminal size of the channels which may decrease the axonal regeneration in terms of number of myelinated axons (Henry et al., 1985).

2. OBJECTIVES

The major goals of this research are the following:

1. To choose an appropriate material for the multiple lumen nerve regeneration cuff; it must be nonimmunogenic, noncarcinogenic, nontoxic, biocompatible, biodegradable (mechanical integrity should be maintained at least for three to four weeks in order to provide time for axonal regeneration [Williams et al. 1983]), ductile enough to suture and permit bending *in vivo*, and if possible, commercially obtainable;
2. To design a cuff with the appropriate dimensions for use *in vivo*; it must provide orientation, mechanical support, guidance for the generating axons, and prevent the invasion of scar tissue (Daniel, 1991);
3. To develop a method to fabricate various such cuffs; and
4. To make several prototype cuffs.

3. LITERATURE REVIEW

3.1 Background

3.1.1 The peripheral nerve in mammals

Mammalian peripheral nerves are cable-like structures consisting of nerve fibers, supportive connective tissue, ectodermally derived supportive cells, blood vessels, and lymphatic vessels.

The functional unit of a peripheral nerve is the nerve cell. The nerve cell consists of the cell body or soma from which cystoplasmic extensions (the dendrites and the axon) originate. Each axon may divide into side branches along its course, or ramify before its termination at the sensory end organ or motor end plate, or both. The axon is surrounded by a plasma membrane of a glial cell, the Schwann cell. There are two main axon types; myelinated and unmyelinated. In the case of unmyelinated axons, the plasma membrane of one Schwann cell can engulf several axons. However, in the case of myelinated axons, the plasma membrane of one Schwann cell is wrapped spirally around one axon, producing a myelin sheath in a portion of the axon. The wrapping is com-

plete except at the nodes of Ranvier, where adjacent Schwann cells almost contact one another and the axons are exposed.

The supportive connective tissue layers that surround the peripheral nerve are the endoneurium, perineurium, and epineurium. The endoneurium is the innermost layer and surrounds the axons and their Schwann cells. This layer is composed of collagen fibrils, fibroblasts and blood vessels. These collagen fibrils contribute to the elasticity of the nerve. The next layer is the perineurium that encircles the endoneurium, forming individual fascicle. This layer is made of an outer sheath of dense collagen fibers (perpendicular to the nerve axis) and an inner sheath of multiple layers of flat squamous cells (perineurial epithelium). Several of the functions of the perineurium are the following: active transport of material by pynocytic vesicles present in the cytoplasm of the perineurial epithelium cells and as a diffusion barrier between the fascicle and extra-fascicle contents. In addition, the perineurium maintains the positive pressure inside the fascicle and gives structural support for the neural tissue. The last layer is the epineurium that binds and supports the nerve fascicles together to form the peripheral nerve. This layer consists of loosely arranged, collagen bundles, blood vessels and lymphatics (Daniel and Terzis, 1977; Martini, 1989). See Figure 3.1 for a schematic representation of a mammalian peripheral nerve and related structures (from Junqueira and Carneiro, 1980; page 170).

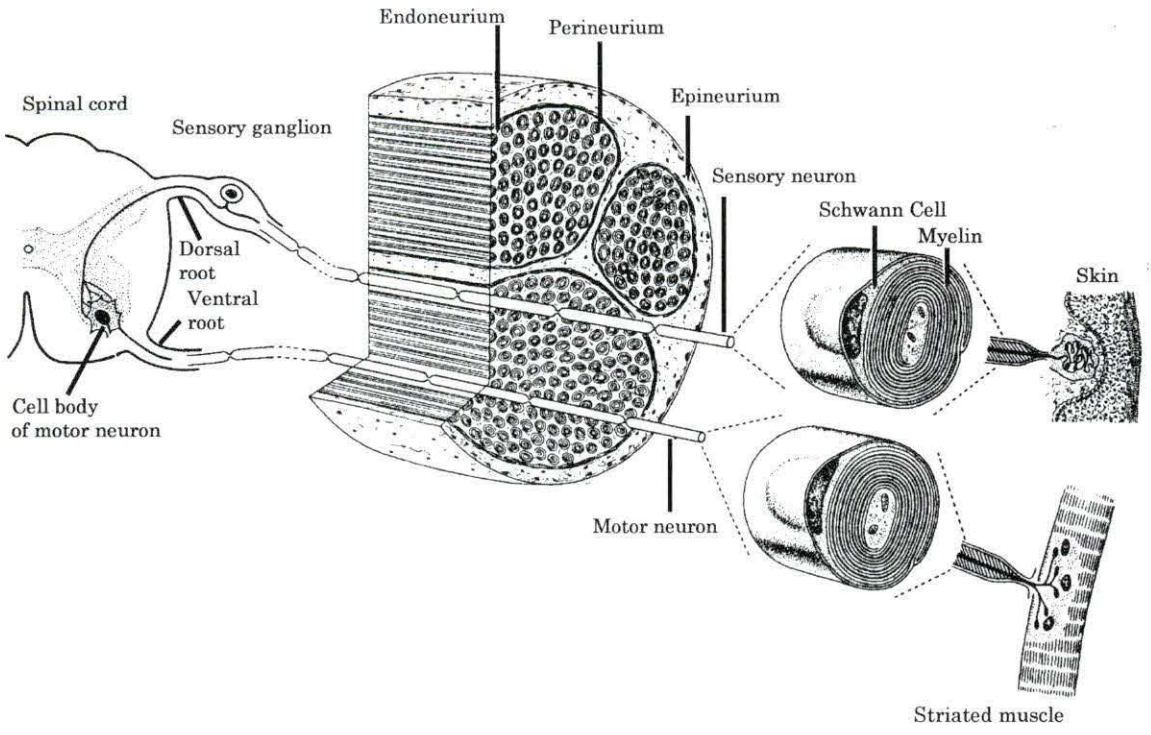

Figure 3.1: Schematic representation of a mammalian peripheral nerve and related structures (Junqueira and Carneiro, 1980)

3.1.2 Peripheral nerve degeneration

A peripheral nerve has the opportunity to regenerate if the cell body is not destroyed. In addition, the recovery of a damaged nerve depends on the distance from the site of the lesion to the cell body. It has more chance to recover if this distance is longer. Also, the healing of a damaged nerve is dependent on the location of the damage or transection, the gap between the proximal and distal

sections, the alignment of the nerve stumps, and the damage and hemorrhage from the surrounding tissues.

When a peripheral nerve is transected, degenerative and regenerative changes occur almost at once. Directly after transection, hemorrhage and clotting appear between the nerve stumps. Also, noticeable swelling of the cut ends (about 7.5 mm from the point of transection) occurs within the first hour of the injury event, and gradually recedes during one week after this event. This swelling is due to accumulation of serum and plasma and mucopolysaccharides. The proximal segment of the transected site preserves its continuity with the cell body (trophic center) and commonly regenerates. However, in the case of extensive damage to the nerve, traumatic degeneration in the proximal site may extend beyond the first nodes of Ranvier to several centimeters. The distal segment that is separated from the source of nourishment (cell body) undergoes Wallerian degeneration that is more extensive than for the proximal site. This degenerative process can reach the neuromuscular junctions in about three to five days after transection and leave them non-functional.

The proximal end of the distal stump is isolated from the rest of the distal stump and survives (no evident degeneration) for about 2 weeks. However, for the remaining parts of the distal stump, the axonal and myelin degeneration is evident 2 days after transection. In this process, the axoplasm clusters and in-

creases in optical density. In addition, the myelin sheath loses its layered arrangement and turns into a compartmentalized (elliptical sections) homogeneous mass that surrounds the axonal remains. However, some of the connective tissue and the perineurial sheaths are left intact in this degenerative process. The removal of the axonal and myelin breakdown products is done by macrophages (intraneural and extraneural) and phagocytic Schwann cells. This phagocytic process begins 7 days after transection and lasts about 3 to 8 weeks (with a peak in phagocytic activity at 3 weeks). While these processes are taking place, the Schwann cells multiply inside the remaining perineurial sheaths in an orderly fashion, forming solid cellular columns that serve as guides for the regenerating axons. However, if these regenerated axons are misrouted and do not invade the distal stump, the distal stump contracts and is replaced by connective tissue (Swaim, 1987; Junqueira and Carneiro, 1980). See Figure 3.2 for details of peripheral nerve degeneration (after Swaim, 1987; page 496).

3.1.3 Peripheral nerve regeneration

In regeneration of a peripheral nerve, the regenerated axons grow from the proximal stump into the distal stump. This process begins inside the cell body of the damaged neuron. Some of the physical changes that occur in the cell body are the following: chromatolysis (dissolution of the Nissl bodies [mitochondria, ribosomes, and other cell organelles]), migration of the nucleus to the cell body

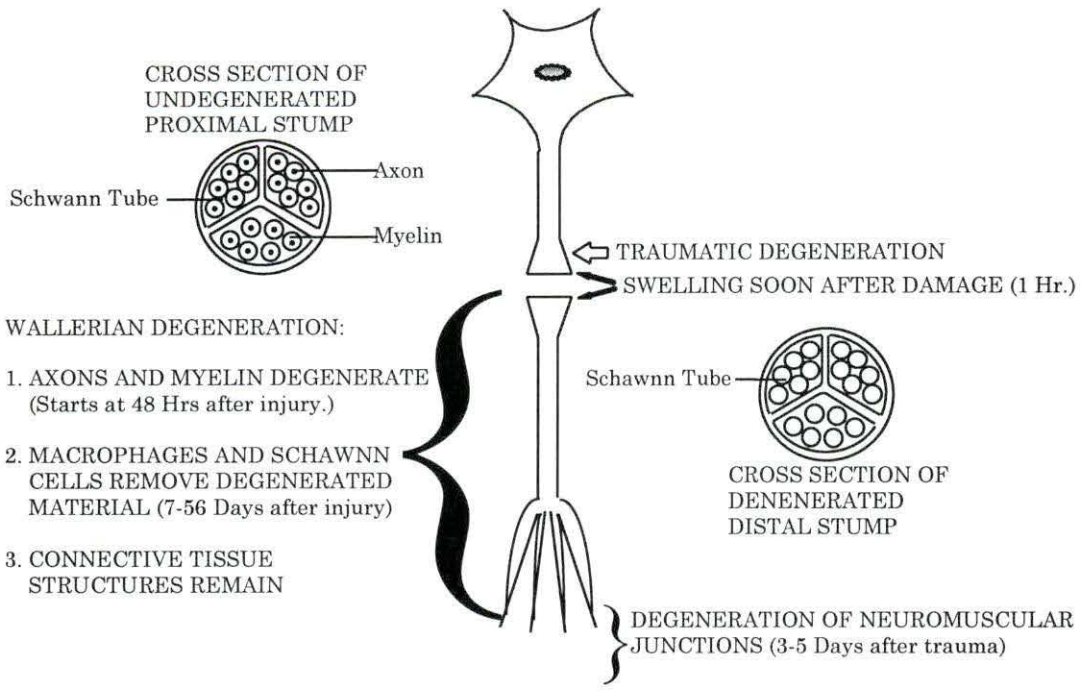

Figure 3.2: Summary of peripheral nerve degeneration (Swaim, 1987)

periphery, and an increase (peaks early in regeneration and when neuromuscular junctions are formed) in the cell body volume. During active regeneration, there is an increase in deoxyribonucleic acid (DNA) and ribonucleic (RNA) activity that produces an increase in enzymatic activity and protein production. The amount of protein and other synthesized anabolic products in this process is about 50-100 times of the amount of these synthesized products for the pre-regeneration state. The metabolic activity and energy expenditure associated with nerve regeneration increase if the damaged site is relatively closer to the cell body. Furthermore, if the injury is too close to the cell body and the nerve

cell survives, the metabolic capacity of the nerve cell may not be enough to cause axonal regeneration along the length of the distal stump. The newly synthesized products (protein and other anabolic products) migrate distally through the axoplasm by two transport mechanisms, microperistalsis within the nerve trunk membrane (at 1 mm/day) and transportation in microtubules (100 mm/day). The fast transport in microtubules is the primary mechanism for satisfying the increase in nutritional requirements and metabolic activity at the synaptic regions.

At the proximal and distal stumps, the endoneurial and epineurial connective tissue, Schwann cells and capillaries begin to proliferate within 1 to 3 days after nerve transection. The result of this process is the formation of a tissue bridge and a capillary bed in which the regenerating axons from the proximal stump can reach the distal stump. The proliferation of Schwann cells greatly outnumbers that of the connective tissue cells of endoneurial and perineurial origin. In the proliferation of Schwann cells, the Schwann cells tend to arrange longitudinally (forming the bands of Büngner), migrate toward each other and join together from the pre-formed Schwann tubes of each nerve stump.

Four to twenty days after the nerve injury, axon sprouting can occur from the proximal stump. These axons have a natural affinity with the bands of Büngner (homotropism) and can follow these bands across the injury site into

newly formed endoneurial tubes (most of the time) or pre-formed endoneurial tubes in the distal stump. Remyelination of the regenerating axons occurs at the injury site as in the distal stump. However, only the axon branches that contact the peripheral end plate are myelinated.

The axonal regeneration is an unsteady process with slowing periods at the beginning and end of the regeneration. In the early stages of this process, it can progress at 0.25 mm/day. After this initial lag period, the rate of axonal regeneration is about 3-4 mm/day (slower at the more distal regions [Swaim, 1987; Junqueira and Carneiro, 1980]). However, the rate of functional return is about 1-2 mm/day. See Figure 3.3 for details of peripheral nerve regeneration (Swaim, 1987).

3.2 Nerve repair techniques

3.2.1 General

There are two basic nerve repair techniques used currently; the conventional suture technique (end-to-end anastomosis) and the nerve bridge technique. When the nerve gap is 10 mm or less, the conventional suture technique is used. However, if the nerve gap varies from 10 mm to 50 mm, the nerve bridge technique is used. The nerve autograft is the ideal repair technique in this case because it is non-immunoreactive, it serves very well as a passive con-

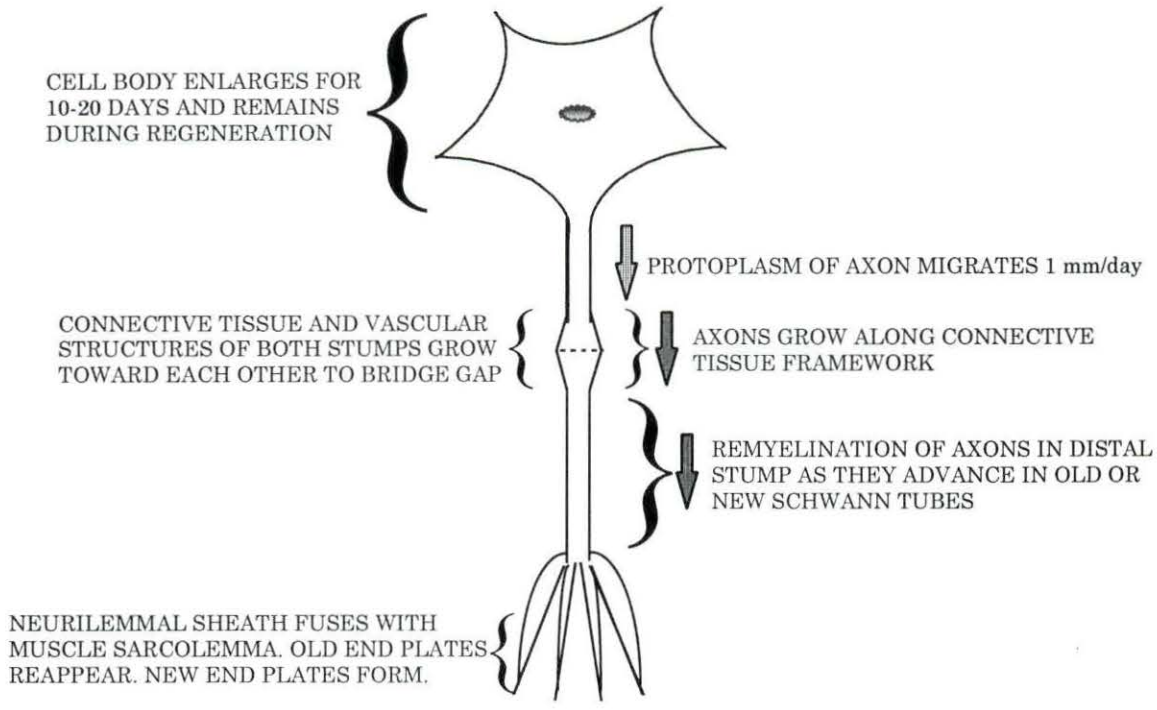

Figure 3.3: Summary of peripheral nerve regeneration (Swaim, 1987)

duit for axonal regeneration, and it has a well-developed vascular bed. However, some inconveniences of this technique are the lost of function in the area where the donor nerve is taken and the increased risk of further surgery. Thus, an alternative nerve bridge technique, such as artificial nerve grafting, may be used instead. The artificial nerve graft must meet the same criteria as those for the nerve autograft. In addition, an ideal artificial nerve graft should be biodegradable to permit, if possible, a full maturation of the nerve and to maintain its in-

tegrity as a guide and mechanical support over the time that it takes for the injured nerve to regenerate (Rosen et al., 1989; Pham et al., 1991).

These two types of nerve repair techniques can be further classified into two basic methods: the anatomical method (nerve connective tissue layers are adjacent in the repair site) and the cellular method (nerve connective tissue layers are separated in the repair site) The following sections present examples of several investigations that emphasize each of these methods.

3.2.2 Past research summary

In the literature (regarding the anatomical method of nerve repair), it is found that some of the studies of nerve regeneration have used rat sciatic nerve as an animal model (Williams et al. [1983, 1987]; Satou et al. [1986]; Knoops et al. [1990]; Guénard et al. [1991]; Maeda et al. [1993]; Hanson et al. [1994]). Some of these studies have used a silicone rubber cuff (Williams et al. [1983, 1987]; Satou et al. [1986]; Maeda et al. [1993]; Hanson et al. [1994]) as the artificial nerve graft.

From these works, Williams et al. [1983] studied the spatial-temporal progress of peripheral nerve regeneration within a silicone chamber and concluded that a regenerated nerve can bridge a nerve gap of 10 mm in four weeks. It was shown (as measured by histological studies) by Satou et al. [1986] that with a very fine collagen (Cell Matrix II [0.3%]; source: Nitta Gelatine Co., Ltd., Osaka,

Japan) added to the inner lumen of a silicone rubber tube, the control of the direction and orientation of the axonal regeneration in that tube is better than that found using an empty silicone rubber tube. Also, Guénard et al. [1991] indicated (as measured by histological studies) that a smooth surface in the inner lumen of the silicone rubber tubes is necessary for the formation of a discrete regenerated nerve cable and that it is possible to have the formation of multiple discrete cables in multiple-compartment silicone rubber tubes. In addition, Maeda et al. [1993] found (as measured by histological and electrophysiological studies) that through sequentially alternating silicone rubber tubes and nerve grafts ("stepping-stone grafts"), regenerated nerves can bridge across long gaps (18-24 mm). However, autografts can bridge this gap with regenerated nerve with better conduction velocities.

Also, in the anatomical method of nerve repair, biodegradable nerve cuffs have been used. Essentially, the advantages of using the biodegradable nerve cuffs are that after nerve regeneration is achieved, the material is biodegraded. Therefore, a second operation is not necessary to remove the material, and in many cases (as with polylactic acid polyglycolic acid) the tissue response to the material is minimal (Nyilas et al., 1983; Rosen et al., 1992). Some of the animal models for nerve regeneration (using biodegradable nerve cuffs) have been rat peroneal nerve (Rosen et al. [1990, 1992]; Keely et al. [1991]; Pham et al.

[1991]), rat sciatic nerve (Seckel et al. [1984]; Zellem et al. [1989]; Hoppen et al. [1990]; Den Dunnen et al. [1993]), mouse sciatic nerve (Nyilas et al. [1985]; Henry et al. [1985]; Da Silva et al. [1985]; Madison et al. [1985, 1987]), and monkey ulnar nerve (Dellon and Mackinnon [1988]). However, few clinical trials have been done using biodegradable nerve cuffs. In one clinical trial (Mackinnon and Dellon [1990]), polyglycolic acid tubes were used in human digital nerves (these tubes were interposed in these injured nerves which had 5-30 mm nerve gaps) with a relatively successful outcome (only 14% showed functional failure).

Some of these works that used rat peroneal nerves investigated the axonal regeneration (as measured by histological and electrophysiological studies) through polyglycolic acid and glycolide trimethyl carbonate biodegradable tubes (both tubes filled with collagen) and autografts. It was found that the parameters to assess the quality of nerve regeneration (the conduction fraction, number of myelinated axons, and axonal organization) were similar in all the graft types utilized.

In studies with rat sciatic nerves, it was shown (as measured histologically) that the distal stump exerted an important trophic effect on axons in the proximal stump (i.e., axonal regeneration) with nerve gaps of 10 mm or less and that well-vascularized nerve cables are formed with minimal tissue reaction

through D,L-PLA tubes (degraded in three months) [Seckel et al. (1984)]. In addition, a biodegradable two-ply nerve cuff (L-PLA/PCL, with an external macroporous layer [more biodegradable than the other layer] and an inner dense layer) was compared for axonal regeneration (as measured by histological and electrophysiological studies) with a sutured autograft. Here similar conduction velocities and number of myelinated axons were observed in both graft types (with minimal tissue response). It was concluded that the axonal regeneration through the L-PLA/PCL was as good as that through the autografts (Hoppen et al., 1990).

In the mouse sciatic nerve model (in the anatomical method of nerve repair), some investigators have used biodegradable (D,L-PLA, molecular weight varying from 20,000 to 100,000) tubes (usually plasticized with 2 to 10% triethyl citrate). In these studies, minimal tissue reaction to the D,L-PLA tubes was found (Nyilas et al. [1985]; Henry et al. [1985]; Da Silva et al. [1985]; Madison et al. [1985, 1987]). In the studies of Nyilas et al. [1985] and Henry et al. [1985], their use was successful (as established by the presence of well-vascularized regenerated nerve cables and number of myelinated axons across the repair site) for nerve regeneration (nerve gaps of 3 to 5 mm) in 60 to 100% of the grafts using D,L-PLA tubes. Here, the nerve regeneration took place in three to six weeks. Also, Henry et al. (1985) found that when the nerve guide

inner lumen is decreased (less than 0.5 mm) and the nerve guide biodegradability is increased (percent of triethyl citrate > 5), the distortion and the probability of occlusion of the inner lumen is increased with a concomitant reduction in the axonal regeneration. Da Silva et al. (1985) have shown similar results (compared to those of the Nyilas et al. [1983] and Henry et al.[1985] studies) for nerve regeneration across a nerve gap of 5 mm through D,L-PLA tubes with similar inner lumen dimensions. However, it was shown that the number of labeled (retrogradely labeled with horseradish peroxidase in a retransection procedure distal to the repair site) nerve cell bodies (dorsal root ganglia and ventral horn) found at the different evaluation times (after initial implantation) is a more precise measure in the assessment of axonal regeneration than the number of myelinated axons, because of axonal branching at the early stage of nerve regeneration. Here, a differential axonal regeneration occurred in which a greater percentage of motor axons regenerated than sensory axons. In addition, Madison et al. (1985, 1987) have found that laminin has an enhancing effect (as measured by number of myelinated axons and horseradish peroxidase-labeled nerve cell bodies) in the early stages of nerve regeneration when laminin filled-D,L-PLA tubes are used as artificial nerve grafts. A well-vascularized nerve cable was found two weeks after initial implantation in laminin filled-D,L-PLA tubes, but not in empty D,L-PLA tubes. However, at six weeks, the number of

myelinated axons and labeled nerve cell bodies were higher in the animals with empty D,L-PLA tubes than in those with laminin filled-D,L-PLA tubes. The explanation for this outcome is that laminin may accelerate the biodegradation and reduction of the luminal size with a concomitant reduction in axonal regeneration. Therefore, it was concluded that the initial delay in the early stages of axonal regeneration does not preclude the axonal outgrowth at later times.

In relation to the cellular method of nerve repair, a study has been done using the rat sciatic nerve model with silicone rubber multiple lumen cuffs as the artificial nerve graft (Daniel, 1991). Also, various studies have been done using the rat peroneal nerve model with polyglycolic acid tubes as biodegradable nerve grafts (Rosen et al. [1983]; Marshall et al. [1989]). Finally, work has been done using the primate ulnar nerve model with biodegradable (polyglycolic) nerve cuffs (Hentz et al. [1991]).

The use of a multiple lumen cuff (silicone rubber) was one of the first attempts to use a multiple lumen compartment which at the same time separated the different nerve connective tissue layers in the nerve regeneration (Daniel, 1991). This study compared (as measured by histological studies) the nerve regeneration across a 5 mm nerve gap through a silicone rubber multiple lumen cuff, a silicone rubber single lumen conduit, and use of just an epifascicular suture technique at the repair site (no nerve gap). Minimal to moderate tissue re-

action was seen in the silicone single lumen cuff and the multiple lumen cuff experiments. The mean axon diameters, axonal cross section areas, and total nerve cross sectional areas were similar in the three nerve repair techniques. However, seven discrete nerve cables were seen through the multiple lumen conduits (one nerve cable for each lumen) compared with a single fascicle through the single lumen cuff, and the repair site utilizing the epifascicular suture technique. It was concluded that the multiple lumen cuff can support, guide, and orient nerves regenerating across a 5 mm gap in a rat sciatic nerve.

In the studies using rat peroneal nerve for nerve regeneration (across a nerve gap within 1 mm), fascicular tubulization (with polyglycolic acid) was compared with fascicular suture technique (Rosen et al. [1983]). The tissue response was minimal. The axonal organization in the fascicular tubulization was better compared to the axonal organization in the fascicular suture technique. In addition, the mean axon diameter and axonal count were similar in both techniques.

For the study using the primate ulnar nerve for nerve regeneration (across a nerve gap of 1 mm), fascicular tubulization (with polyglycolic acid) was compared with fascicular suture technique (Hentz et al. [1991]). The conduction fraction, mean axon diameter and axonal organization were similar among the techniques used. It was concluded that nerve regeneration seen in the fascicular

tubulization with polyglycolic acid is as good as that seen using the fascicular suture technique.

3.2.2.1 Anatomical method

The two conventional suture techniques (epifascicular and fascicular) and the epifascicular tubulization are examples of the anatomical method. The different nerve tissue layers (epineurial, perineurial, and the neural parts of the fascicle) are contiguous in the repair site. Therefore, the fibroblasts of the epineurial layer may invade the neural parts of the nerve, diminishing the axonal regeneration.

3.2.2.1.1 Non-biodegradable cuff

The non-biodegradable materials that were used as nerve guides in the works that are to be discussed in the subsequent paragraphs are the following: impermeable silicone rubber tubes with or without added substances (e.g., collagen, laminin) on the inner lumen, impermeable silicone rubber tubes with different surface textures, impermeable silicone rubber tubes with a low direct current, combination of nerve autografts and impermeable silicone rubber tubes, and acrylic semipermeable tubes.

In 1983, Williams et al. used rat sciatic nerves to study spatial-temporal progress of peripheral nerve regeneration across a 10 mm nerve gap through a

silicone rubber tube of 1.2 mm in internal diameter (ID). The morphologic evaluations were for samples representative of 1 week, 2 weeks, 3 weeks, and 4 weeks after the initial transection. In all time intervals, the average diameter for the conical formed central tube (across all the gap) at 1 mm and 7 mm from the proximal stump was about 0.6 mm (50% of the diameter sizes of the proximal and distal stump [1.2 mm]) and 0.3 mm (25% of the diameter sizes of the proximal and distal stump [1.2 mm]), respectively. At 2 weeks, a central fibrin matrix tube (the nerve gap was bridged at 1 week) was entirely invaded by fibroblasts and Schwann cells from both nerve stumps. At this time, non-myelinated axons were invariably seen at 2 to 3 mm from the proximal stump. At the third week, the nerve gap was crossed by fibroblasts, Schwann cells, and blood vessels. Also, at this time, non-myelinated and myelinated axons were consistently observed at 9 mm and 3 mm respectively from the proximal stump. In the last time interval (fourth week), non-myelinated axons bridged the gap, and the myelinated axons were commonly seen at a distance of 7 mm from the proximal stump. At this time, a perineurial-like layer was also observed across the gap. In summary, the observations suggested that in this silicone chamber the first event in nerve regeneration is the accumulation of fluid that is converted (in part) into a fibrin matrix that is axially oriented in the center of this chamber. This fibrin matrix is subsequently invaded by non-neuronal cells

(fibroblasts and Schwann cells) that in turn serve as a substrate for the regenerating axons. These regenerating axons then are progressively myelinated from the proximal side of the nerve lesion to the distal side. The position of the myelinated axon front appears at comparable locations three to five days following the non-myelinated front development.

In a study with rats, Satou et al. (1986) examined the effects of a collagen gel matrix (consists of a solution of very fine collagen fibers, Cell Matrix II [0.3%]; source: Nitta Gelatine Co., Ltd., Osaka, Japan) on nerve regeneration. They interposed silicone rubber tubes between the distal and proximal stump of severed sciatic nerves, forming a 5 mm gap. The test silicone rubber tube was injected with collagen gel (Cell Matrix II, 0.3%), and the control tube received no injection. In the histological analysis, from the 14th to 17th day of the initial implantation, an initial sprouting of axons was found in the test specimens with few fibroblasts and Schwann cells. However, in the control specimens, Schwann cells and fibroblasts (particularly) were more abundant and less organized than in test specimens. By the fourth week, fine, sprouting axons were found in the distal part of the test specimens, but not in the control specimens. On the 35th day, the axons in the central portion were mostly myelinated in both test and control specimens. However, sprouting axons were found well beyond the distal stumps of the test specimens. Satou et al. (1986) concluded that silicone rubber

tubes filled with a collagen gel (Cell Matrix II, 0.3%) are better than empty silicone rubber tubes in controlling the direction of the proliferating Schwann cells, in stimulating initial axonal sprouting, and in discouraging propagation of fibroblasts.

In 1987, Williams et al. used rat sciatic nerves to compare three methods of nerve repairs: an empty silicone rubber chamber (control), a silicone rubber chamber filled with phosphate-buffered saline (PBS), and a silicone rubber chamber filled with dialyzed plasma (DP). The nerves were transected and the chambers interposed between the distal and proximal nerve stump, forming a 15 mm gap. The chamber internal diameter was approximately 1.8 mm (average nerve diameter = 1.2 mm). In the morphological analysis, at 1 week, a thin fibrin matrix was found in the empty chambers, but a thick fibrin matrix was found in the PBS-filled chambers (no morphological analyses were made for the DP-filled chambers at 1 week and 4 weeks). At 4 weeks, no nerve structure was found in the empty chambers, but 33% of the intact PBS-filled chambers had regenerated axons cross the chamber gap. At 8 weeks, no regenerated nerve or structure was found in the empty chambers, but 71% of the intact PBS-filled chambers and 57% of the intact DP-filled chambers had regenerated nerves cross the chamber gap. However, in comparison to the anterior filled chambers, only 20% of the PBS-filled chambers had myelinated axons reaching the distal

parts, whereas 100% of the DP-filled chambers showed that myelinated axons crossed the gap. In addition, there was no statistical difference in the average regenerated nerve diameters between those of PBS or DP filled chambers. The electromyography analysis showed lower amplitudes in animals with both types of filled chambers compared to those with normal sciatic nerve. Forty-three percent of the rats with intact DP-filled chambers had an action potential compared with the presence of an action potential in 14% of the rats which had intact PBS-filled chambers. Also, Williams and co-workers concluded that nerve regeneration is dependent on other factors such as the quality and homogeneity of the fibrin matrix. They proposed that the DP-filled silicone rubber chamber is much better for nerve regeneration (mainly due to myelinization of axons) because the DP-filled silicone rubber chamber probably has a more homogeneous fibrin matrix or that the fibrin matrix appears in amounts in DP-filled silicone rubber chambers more conducive to the cellular migration compared to the PBS-filled silicone rubber chambers.

In 1991, Guénard et al. designed a study to determine how regenerated nerve morphology is affected by using two-compartment silicone rubber nerve guides with different surface textures in the hydrophilic or hydrophobic partition walls. The different partition wall textures and compositions were the following: 1) rough nitrocellulose (R-NC, hydrophilic), 2) smooth nitrocellulose (S-

NC, hydrophilic), 3) rough polyvinylidene fluoride (R-PVDF, hydrophobic) and, 4) smooth polyvinylidene fluoride (S-PVDF, hydrophobic). The nerve guides were interposed between rat sciatic nerve cut ends (forming a 10 mm gap between the ends) and were examined after four weeks of implantation. Regenerated nerves were seen in all the nerve guides except the S-PVDF where only 60% of the animals had regenerated nerves. In each one of the nerve guides with rough membranes, two bell-shaped nerve cables (one cable for each compartment of the nerve guide) were found adhered to the partition wall by means of a macrophage cell layer. In contrast, for the nerve guides with smooth membranes, fifty percent of these nerve guides (each one of them) had two round nerve cables (one free-floating cable for each compartment of the nerve guide), but the other fifty percent did not have any regenerated nerve cable. In all the regenerated nerves, there were numerous microfascicles that were delineated by perineurium and surrounded by a epineurial layer. These microfascicles consisted of myelinated axons, unmyelinated axons, and Schwann cells. The number of myelinated axons were similar in all the nerve guides (R-PVDF = 1806 ± 345, R-NC = 1348 ± 452, S-PVDF = 1989 ± 428) except in the S-NC guides (592 = ±185) which had a much lower number. In addition, the epineurium thicknesses facing the partition wall were similar in all the nerve cuffs (R-NC = 52.2 ± 6.4 μm, S-PVDF = 44.1 ± 5.8 μm, S-NC = 63.9 ± 17.9 μm)

except in the R-PVDF tubes (22.1 ± 3.3 μm). Finally, this study demonstrated that the morphology of the regenerated nerve can be controlled by the inner lumen surface texture independent of chemical composition and that two discrete nerve cables can be formed from a single peripheral nerve through a two-compartment silicone rubber tube with a smooth strip used as a partition wall.

In 1990, Knoops et al. compared two types of nerve guides, an acrylic semipermeable (molecular weight cut off, 50,000 daltons) versus a silicone rubber impermeable tube, by using the epifascicular technique in transected rat sciatic nerves that had a 4 mm gap between the cut ends. After two weeks of implantation, a regenerated nerve was seen across the nerve gap through all the semipermeable tubes. In these tubes, the proximal nerve stump (3 mm from the stump) had large and small myelinated axons, but only unmyelinated axons were seen at the mid-portion of the nerve gap and distal stump (2 mm from the stump). However, one week later, all the semipermeable guides had myelinated axons in middle of the gap and in the distal stump. From 5 to 27 weeks, poor fiber organization was observed in the proximal nerve stump of the semipermeable guides, also some fiber branching was noted in the mid part of these tubes. In addition, the myelinated axons did grow larger in this span of time, but their axon diameters were smaller than of those seen in intact nerves. The number of myelinated axons leveled-off after the fifth week of implantation (about 7,000 in

the middle of a tube and about 11,000 in the distal stump) except for those in the proximal stump. These continued increasing until the 27th week (approximately 20,000). Knoops et al. indicated that fiber branching could have occurred and have been maintained from the middle of the nerve gap to the distal stump and that retrograde growth could be the cause for the large count of myelinated axons in the proximal stump. In comparison, they found that after 27 weeks, the number of myelinated axons in the middle of the nerve gap was significatively higher for the impermeable tubes than for the semipermeable tubes (10,000 versus 7,000, approximately). In regard to this, they suggested that the lower number of myelinated axons for the semipermeable tubes compared to the impermeable tubes could be due to the loss of trophic factors through the tube wall pores. Finally, they concluded that for the same tube dimensions and initial tube environment, the tube wall porosity at the molecular level can influence the result of peripheral nerve regeneration.

In 1993, Maeda et al. studied nerve regeneration in transected rat sciatic nerves (right side) across gaps of 18 mm to 24 mm through sequentially alternating silicone rubber tubes and natural nerve grafts ('stepping-stone grafts'). Two types of stepping-stone nerve grafts (group II, 18 mm gap and group III, 24 mm gap) were used and the results obtained with them were compared with those of natural nerve grafts (group I, 18 mm gap), with one silicone rubber

tube (group IV, 18 mm gap), and with normal nerves. In group II (single stepping-stone nerve grafts [SS], one nerve graft between two silicone rubber tubes), the alternating sequence across the 18 mm nerve gap was as follow: proximal nerve stump sutured to a silicone rubber tube (SR I) of 8 mm in length (forming a gap of 6 mm), the SR I is then sutured to a nerve graft (NG I) of 6 mm in length (forming a second gap of 6 mm), then, the NG I is sutured to a second silicone rubber tube (SR II) of 8 mm in length (forming a third gap of 6 mm), and finally, the SR II is then sutured to the distal nerve stump. The conduits were sutured with a 1 mm inset. Likewise, the alternating sequence in group III (double stepping-stone nerve grafts [DS], two nerve grafts between three silicone rubber tubes) across the 24 mm nerve gap was as follow: proximal nerve stump sutured to a silicone rubber tube (SR I) of 8 mm in length (forming a gap of 6 mm), the SR I is then sutured to a nerve graft (NG I) of 6 mm in length (forming a second gap of 6 mm), then, the NG I is sutured to a second silicone rubber tube (SR II) of 8 mm in length (forming a third gap of 6 mm), then, the SR II is sutured to a second nerve graft (NG II) of 6 mm in length (forming a fourth gap of 6 mm), the NG II is then sutured to a third silicone rubber tube (SR III) of 8 mm in length (forming a fifth gap of 6 mm), and finally, the SR III is then sutured to the distal nerve stump. Regenerated nerves were found through the implants in all the groups except in group IV (one silicone rubber

tube). In the quantitative histological analysis, group I and group II had a similar histological pattern of well-myelinated axons (group I = 3,500 ± 2,000 and group II = 4,500 ± 5,000 axons) and microfascicle-like structures compared to a decreased number of myelinated axons for regenerated nerves in group III (2,000 ± 2,500). However, these experimental groups had a lower amount of myelinated axons than that found for the normal nerves. In addition, myelinated axons in group I and group II had similar diameters (group I = 4.3 ± 0.7 μm, and group II = 3.5 ± 0.5 μm), and these were greater than those found in group III (2.0 ± 1.5 μm). However, the average diameter of the myelinated fibers of the normal nerves (6.0 ± 0.3 μm) was larger than these averages found in the experimental groups. In the nerve graft and stepping-stone groups, a minimal functional restoration of the muscle of the legs was found after 16 weeks of the initial implantation. It varied from about an average of 10% for group II and III (stepping-stone nerve grafts) to about an average of 25% of the normal function for the nerve graft group. This difference in the recovery of the function between the nerve graft group and the stepping-stone nerve graft groups was not significant. In the electrophysiological analysis, the conduction velocities for the nerve graft group (about 43 m/s) were higher than those found for the stepping-stone groups (about 28 m/s). The regenerated nerve conduction velocities found for these experimental groups were lower than that found for the normal nerves

(about 59 m/s). Finally, Maeda et al. concluded that the interposition of nerve grafts between nerve guides (stepping-stone nerve graft technique) can enhance the nerve regeneration across long nerve gaps (18 to 24 mm) in comparison to a single long conduit of silicone rubber with similar nerve gaps.

In 1994, Hanson and McGinnis examined the effect of direct current of 10 μA on transected rat sciatic nerves inside silicone rubber tubes. The gap formed between the nerve ends was 5 mm. These silicone rubber tubes were pierced at the midpoint of the nerve gap by stimulating and sham (control = no stimulation) cathodes. The cathode wire was curved into a loop along the inside circumference of the wall of the silicone rubber tube. After 3 weeks of continuing electrical stimulation, only 35% of the stimulated transected nerves had myelinated axons in the gap center (axonal count = 1656 ±607) compared to 100% myelinated axons for the non-stimulated nerves (axonal count = 4215 ± 412). In addition, there was a gradual reduction of myelinated axons across the gap from the proximal stump (about 4600) to the distal stump (about 3800) for the control nerves. In contrast to this, a sharp axonal reduction (proximal stump 4,500 to distal stump 800, approximately) was found for the stimulated nerves. Also, multioculated cysts (cluster of spaces filled only with fluid) were found in the central portion of the stimulated regenerated nerves. This contrasted with a central dense packed core of myelinated axons for the control nerves. The re-

searchers concluded that the application of low direct current, as used in this study, inhibits peripheral nerve regeneration. In addition, they proposed that electrolysis products (as H_2 and OH^-) could have caused the aberrant cystic formation and the sharp reduction in myelinated axons across the gap (especially in the nerve gap center).

3.2.2.1.2 Biodegradable cuff

The biodegradable materials that were used as nerve guides in the studies that are discussed in the subsequent paragraphs are the following: glycolide trymethyl carbonate tubes with or without collagen (on the inner lumen), polyglycolic acid tubes with or without collagen (on the inner lumen), copolymer tubes of polyglycolic/polylactic acid, semipermeable copolymer tubes of polycaprolactone/polylactic acid, copolymer tubes of Kreb's cycle compounds, and empty polylactic acid tubes (usually plasticized with triethyl citrate) or with collagen, laminin or fibrinogen (among other substances) on the inner lumen.

Rosen et al. (1992) used rat peroneal nerves to compare two nerve bridge techniques: the sutured autograft nerve (SAG) and the artificial nerve graft (ANG). This artificial graft was made of a bioresorbable material (glycolide trimethyl carbonate, GTMC) filled with collagen. For the SAG, a 5 mm segment of the peroneal nerve was removed, forming a 5 mm gap in the nerve. Then, the peroneal nerve autograft from the opposite side was sutured to the transected

peroneal nerve. For the ANG, the GTMC tubes were interposed between the distal and proximal stump of the transected peroneal nerves, forming a 5 mm nerve gap. Six to 9 months after the initial transection, the animals were evaluated using functional analysis (the toe spread pattern when walking), and histology and electrophysiology. In the functional analysis, the results were similar in both repair methods (the distance from the first to the fifth digit [first to fifth toe spread pattern] varied from 1.95 to 2.10 cm when the treated rats walked across an X-ray film). In the electrophysiological analysis (approximately 83 percent conduction fraction [gives the percent of myelinated axons (at the proximal site of the nerve lesion) that had reconnected axons across the repair site]) and in the mean distal axon diameter analysis (approximately 4.2 μm average diameter), the results were similar in both graft types. However, in the axonal count analysis, the SAG had a total number of axons (2,825 axons ± 464) significatively greater than the ANG (2,177 ± 443). The axonal organization (failed [no axonal alignment, 100% neuroma], poor [10 to 39% axonal alignment, extensive neuroma], fair [40 to 69% axonal alignment, moderate neuroma], good [70 to 99% axonal alignment, minimal neuroma], and normal [100% axonal alignment, no neuroma]) at the repair site was fair in both graft types, with minimal or no tissue reaction. Finally, Rosen et al. concluded that the axonal

regeneration was similar in both graft types, but that a higher axonal count was observed for the SAG technique.

In 1989, Zellem et al. used rat sciatic nerves to compare two nerve repair techniques: fascicular suture nerve repair and a nerve repair using polyglycolic acid (PGA) mesh and silicone rubber cuffs. The distal end and the proximal end of a portion of the sciatic nerve were sutured to a pair of parallel ends of a square of rubber or PGA mesh, and immersed in a solution (SOL I composed of chlorpromazine, polyvinylalcohol, NaCl, and KCl, with pH adjusted to 6.4). Then, the nerves were frozen in SOL I (at - 2 °C) and subsequently transected with a vibrating razor. Then, the frozen transected nerves were thawed in another solution (SOL II composed of chlorpromazine, polyvinylalcohol, NaCl, KCl, KH_2PO_4, $NaCO_3H$, and Imidazole, with pH adjusted to 6.8). This solution maintained the homeostasis of the transected nerves. Then, the nerves were bathed in SOL II and realigned with no gap between the nerve stumps. Finally, while bathed in SOL II, the other two parallel ends of the rubber or the PGA mesh were joined to form a tube around the repair site. Two hundred and twenty five days after the initial transection, the functional test for the PGA cuff technique was found to be superior (67 percent of the normal function of the muscles was restored) to the fascicular suture technique (37 percent of the normal function was restored). Also, the histological analysis showed that using the

tubulization technique was better than using the fascicular suture technique. Finally, Zellem et al. concluded that the use of tubulization (providing a reduction of tension in the ends of nerve stumps, maintaining homeostasis, and improving accuracy of alignment by using a sharp cut of the nerves when frozen) showed significant advantages when compared to using conventional suture techniques.

In 1988, Dellon and Mackinnon designed a study to evaluate nerve regeneration in monkey (Macca cynomolgus) transected ulnar nerves using autogenic sural nerve grafts, PGA mesh tubes and PGA rigid (porous) tubes. The PGA mesh and rigid tubes were sutured to the transected ulnar nerves leaving a 30 mm gap between the cut ends. For the autografting technique, three sural nerve grafts (3 cm in length) were interposed and sutured side-by-side between the proximal and distal ends. After one year of implantation, conduction velocity results for the regenerated nerves were similar among the different grafting techniques (about 30 m/s), but they were significatively less than normal control nerves (85 ± 15 m/s). Electromyographic function (in abductor digiti quinti and first dorsal interosseus muscle) was also demonstrated in 60 to 80% of the experimental monkeys with implanted PGA tubes (electromyography was not conducted in animals with implanted autografts). In addition, all the experimental nerve grafts and PGA tubes demonstrated the presence of similar mor-

phological pattern of regenerating axons at the center of the nerve gaps. In the regenerated distal stumps, the total nerve fiber numbers were similar for all test nerves and for the normal nerve (from 13,847 in PGA rigid tubes to 16,172 in autografts). However, the mean fiber diameters were much larger in the normal nerves (6.89 ± 2.66 μm) than in the experimental grafts (PGA rigid tube = 2.81 ± 0.61 μm, PGA mesh tube = 2.95 ± 0.42 μm, and autograft = 4.07 ± 1.76 μm). In light of these results, Dellon and Mackinnon suggested that for short nerve gaps (2-3 cm) the PGA tubes can direct nerve regeneration across these gaps as good as autografts can.

In 1990, Mackinnon and Dellon obtained good clinical results using PGA tubes on affected human digital nerves. The PGA tubes were interposed on the affected nerves to establish nerve gaps of 5 to 30 mm. The patients were evaluated 11 to 12 months after the initial operation. Only 14 percent of the patients exhibited functional failure. Mackinnon and Dellon concluded that their results using the PGA tubes were comparable to those seen when nerve autografts were used.

In 1991, Keeley et al. used rat peroneal nerves to compare two types of artificial nerve grafts: PGA, which is bioresorbable and is non-porous, and HEB (hydrogel-elastomer biopolymer) which is non-bioresorbable and is porous. These artificial grafts were interposed between the distal and proximal stump

of transected peroneal nerves, forming a 5 mm gap. A minimal to moderate tissue reaction to the grafts was observed in the long-term (3 to 6 month survival) animals. In the qualitative histology, the scoring of axonal organization was primarily based on axonal alignment and extent of neuroma (failed [no axonal alignment, 100% neuroma], poor [10 to 39% axonal alignment, extensive neuroma], fair [40 to 69% axonal alignment, moderate neuroma], good [70 to 99% axonal alignment, minimal neuroma], and normal [100% axonal alignment, no neuroma]). The axonal organization at the repair site was good in the PGA tubes, but only fair in the HEB tubes. The quantitative histologic analysis demonstrated similar axonal counts (approximately 3,000) compared to a larger average axon diameter in the HEB tubes (3.7 μm compared to 3.3 μm) in the long-term animals. In conclusion, Keeley et al. demonstrated that the PGA tubes and the high-hydrogel HEB tubes support axonal regeneration in a 5 mm nerve gap, but larger axon diameters were obtained using high hydrogel HEB tubes. Finally, they proposed a follow-up study using the porous non-bioresorbable high-hydrogel HEB tubes and porous-bioresorbable high-hydrogel HEB tubes.

In 1990, Rosen et al. used rat peroneal nerves to compare two bridge techniques: sutured autograft nerve (SAG) and artificial nerve graft (ANG). This artificial graft was made of a bioresorbable PGA tube filled with collagen. For the SAG, a 5 mm segment of the peroneal nerve was removed, forming a 5 mm

gap in the nerve. Then, the peroneal nerve autograft from the opposite side was excised and sutured to the transected peroneal nerve. For the ANG, the PGA tubes were interposed between the distal and proximal stump of the transected nerves, forming a 5 mm gap. They evaluated the axonal regeneration 11 to 12 months after the initial surgical intervention. In both the functional analysis and in the electrophysiological analysis (conduction fraction = 77% ± 12 [SAG] and 82% ± 13 [ANG]), the results were similar (not significatively different) in both grafting techniques (SAG and ANG). In the histological analysis, the mean axon diameter for the SAG was significantly larger (4.49 ± 0.43μm) compared to those results for the ANG (mean axon diameter of 4.19 ± 0.25μm). However, the axonal count (about 3,000 axons) and the axonal organization (fair [40 to 69% axonal alignment, moderate neuroma]) were similar in both graft groups. Finally, Rosen et al. concluded that both PGA tubes filled with collagen and the SAG supported axonal regeneration across a 5 mm nerve gap. Also, they proposed using this type of ANG for longer nerve gaps to test the influence of the collagen.

In 1991, Pham et al. used rat peroneal nerves to compare two repair techniques: epifascicular suture, and epifascicular tubulization (with no gap between the distal and the proximal nerve stump) using PGA tubes + avitene (no suture). The avitene (microfibrillar collagen hemostat, biodegradable adhesive)

was applied around the PGA tube to hold the cut ends of the transected nerve within the tube. Nine months after the initial transection, the electrophysiological analysis demonstrated that the repaired nerves regenerated better with the PGA tubes + avitene (72 ± 18% conduction fraction [gives the percent of myelinated axons (at the proximal site of the nerve lesion) that had reconnected axons across the repair site]) than with the epifascicular suture technique (53 ± 18% conduction fraction). However, in the histological analysis, the mean myelinated-axon count (about 1900) and mean myelinated-axon diameter (about 4.2 μm), showed similar results for both techniques. Finally, Pham et al. concluded that the PGA + avitene holds the nerves as well as the epifascicular suture technique does, and that the axonal regeneration is better with the PGA + avitene than with using the epifascicular suture technique.

Reid et al. (1978) prepared biodegradable nerve cuffs made of copolymers of PGA and polylactic acid (PLA) in order to examine the nerve regeneration in transected ulnar and peroneal nerves of dogs using these cuffs (with no gap between the proximal stump and distal stump). This tubulization technique (with PGA/PLA tubes) was compared with the epifascicular suture technique. The cuffs were custom made with an inside diameter twice that of the diameter of the nerve. The authors indicated that this diameter ratio (cuff inside diameter to nerve diameter) was chosen to avoid or reduce the build-up of neuroma or

connective tissue. These cuffs dissociated completely by 3 months. In the histological analysis, the nerve fiber alignment was seen to be similar to that using the epifascicular suture technique (2.2, of a scale from 1 [good] to 3 [poor]). However, the fibrotic reaction was significatively lower with the biodegradable nerve cuff. In addition, there was a proliferation of connective tissue between the epineurium and the wall of the biodegradable cuff, but no neuroma and only a few inflammatory cells were observed. In the nerve conduction studies, there were no apparent differences observed between procedures. In summary, Reid et al. concluded that the conduction and the nerve fiber alignment results were similar for both techniques. However, there was less fibrotic reaction and no neuroma with the biodegradable cuff. Also, they concluded that the 2:1 ratio between the inside cuff diameter and the nerve diameter does not appear to be the optimal ratio (using these biodegradable cuffs) because of the proliferation of connective tissue between the epineurium and the wall of the biodegradable cuff. They also stressed that this diameter ratio has to be between 1 and 2, and that the optimal diameter ratio is (from a clinical point of view) difficult to achieve.

Molander et al. (1982) used polyglactin meshes (copolymer of PGA and PLA at 9:1 ratio [PGL 910]) to bridge a 9 mm tibial nerve gap in rabbits. These meshes that were composed of multifibered threads (140 μm in diameter) had

an individual pore area of 0.16 mm^2. At the time of implantation, the meshes were preclotted and shaped around the transected nerves and sutured at 3 mm from each cut end. In the gross findings, at 3 weeks after implantation, the tube meshes disappeared. At 6 weeks, the nerve gaps were seen to be bridged by smooth tubes that were non-adherent to the surrounded tissues. While the tube mesh was being absorbed, a connective tissue tube was being formed along with blood vessels, fibroblasts, and collagen. At 16 weeks, this connective tissue tube contained several small fascicles in the center of the tube and minifascicles in its wall. At 16 weeks, remyelination of the axons was very advanced. Finally, Molander et al. demonstrated that polyglactin tube meshes can serve as a framework for the formation of regenerated nerves in 9 mm nerve gaps.

Molander et al. (1983) used transected rabbit tibial nerves to evaluate nerve regeneration across a 10 mm nerve gap using nerve autografts and PGL 910 tube meshes (same implantation procedure as in Molander et al., 1982 to cross the 9 mm gaps). The histological results with the PGL mesh-tube were similar to the Molander et al. (1982) results. However, the nerve grafts were attached to the surrounding tissues with a thick layer of nerve fibers in the new epineurial layer. The myelinated-axon (distal to the nerve injury) diameters (approximately 2.04 $\mu m \pm 0.83$) and the ratios (distal to the nerve injury /proximal to the nerve injury) between the distal and proximal number of mye-

linated axons per mm^2 (approximately 0.75 ± 0.24) were similar in both implant types. Molander et al. (1983) demonstrated that a PGL mesh-tube appears to enclose the regenerated nerve better than the nerve grafts fibers. The PGA tube prevents neuroma formation and adhesion to the surrounding tissues. There were no significant differences in the myelinated axon diameters or myelinated fiber density between the PGA tube or the nerve graft experiments. They concluded that the nerve regeneration through a PGL mesh-tube is as good as through a nerve graft, and the use of a PGA tube offers the advantage that no other nerve is sacrificed.

Hoppen et al. (1990) evaluated nerve regeneration across a 7 mm gap through biodegradable cuffs (internal average diameters of 1.2 to 1.3 mm) and autografts in rat transected sciatic nerves. This biodegradable cuff consisted of a outer macroporous layer (had pore size of 30-70 μm and wall thickness of 250 μm, and was prepared by salt casting and phase separation) made from a mixture of L-PLA (high molecular weight) and polyurethane (PU), and a inner microporous layer (had pore size of 0.5-1 μm and wall thickness of 10 μm, and was prepared by a dip molding technique) made from a copolymer of L-PLA/ PCL (poly-ε-caprolactone). The purpose of the outer macroporous layer was to facilitate the cuff biodegradation and to allow the ingrowth of capillaries through its porous network that could enhance the inflow of nutrients and outflow of accu-

mulating fluids through the inner microporous layer. Also, this inner layer could prevent the ingrowth of perigraft scar tissue. After four weeks of implantation, all the rats were able use their hind legs and there were no plantar ulcers or exposed bones. Stimulation of the sciatic nerve 8 weeks after the initial transection produced ankle motion. In addition, the conduction velocity of the regenerated nerve within the nerve cuffs (50 ± 10 m/s) and the autografts (48 ± 15 m/s) were similar. In the qualitative histologic analysis (after 8 weeks of implantation), a regenerated nerve cable, containing numerous myelinated axons (in the nerve cuff, it was enclosed by a thin fibrous sheath), was observed in all the nerve guides and autografts. No perigraft scar tissue and neuroma were observed inside the nerve cuffs, but more endoneurial scarring was seen in the autografts. In regard to the different cuff layers, the inner layer was intact at the time of evaluation, but the outer layer was partially disintegrated and was subsequently invaded by fibrohystiocytic tissue. Hoppen et al. concluded that this two-ply biodegradable cuff design is as good as the autografts in enabling nerve regeneration across a 7 mm gap. They indicated that this design could be used with other biodegradable systems to optimize biodegradation.

Den Dunnen et al. (1993) evaluated nerve regeneration and maturation through a 10 mm gap of rat sciatic nerve after 24 months of implantation of bioresorbable tubes made of copolymers of L-PLA/PCL (1:1). These tubes

(prepared by a dip coating procedure) had porous outer layers and dense inner layers. The porosity was obtained by mixing the sugar crystals into the polymer solution (L-PLA/PCL [1:1]). There was active plantar flexion with no plantar ulceration or mutilation in all the evaluated animals. In all of the experiments, a regenerated nerve (enclosed by a fibrous capsule and few copolymer particles that were surrounded in turn by a few fibroblasts and macrophages [minimal tissue reaction]) was observed across the nerve gap. The number of myelinated axons per cross section area (in general, standard areas of 530 μm^2 were examined from each cross section) in the proximal stump (315 ± 167 axons), middle of the gap (370 ± 111 axons), and distal stump (315 ± 93 axons) for the regenerated nerves was much higher than that found for normal rat sciatic nerves (130 ± 18 axons). In addition, the equivalent diameters of the myelinated axons in the different histological sections (proximal stump = 5 ± 3 μm, gap middle = 5 ± 2 μm, and distal stump = 4 ± 2 μm) for the regenerated nerves were much lower than that found for the normal rat sciatic nerves (9 ± 4 μm). However, the percentages of axonal myelination ([1-[axonal area/[axonal area + myelin sheath area]]] x 100) were similar in all experimental animals (regenerated nerves, about 36 ± 18%) and controls (normal rat sciatic nerves, about 33 ± 9%). Den Dunnen et al. proposed that a larger number of myelinated axons in the experimental animals could be due to axonal branching after transection of the nerve. They concluded

that this PLA/PCL nerve cuff can bridge a nerve gap of 10 mm (with minimal tissue reaction) with a regenerated nerve (with return of motor function) that has the same relative amount of myelination as the control (normal sciatic nerve) after two years of implantation.

Nyilas et al. (1983) used mouse sciatic nerves to evaluate nerve regeneration using bioresorbable tubes (0.5 to 1.25 mm ID, wall thickness [WT] of probably 0.25 mm, and length of 5 mm) across a 5 mm gap. These tubes were composed of the following: 1) PLA (L and D,L [probably with a MW of 20,000]; source: Polysciences, Inc., Warrington, PA) without plasticizer, with high molecular plasticizer (5% copoly[1,6-hexylene-(1:1)-L-lactate/succinate] (HLA/S) with a MW of 8,000), and with low molecular weight plasticizer (2%, 5% and 10% triethyl citrate, TEC [MW = 276]); 2) 3:1 composite of PGA/poly(2,3-butylene succinate) [PGA/PBS], and 3) 3:1 composite of L-PLA/copoly[1,4-butylene-(2:1)-D,L-lactate/D,L-malate]. All the polymers used for these biodegradable tubes were purified by reprecipitative fractionation. The plasticizers were used to impart flexibility and suturability to the tubes prepared with L-PLA and D,L-PLA which would otherwise be hard and brittle. All the bioresorbable tubes were made by dip-molding using a platinum wire (0.5 mm ID) mandrel precleaned by heating to a white glow. The solvents used in this procedure were acetone and tetrahydrofuran for the non-PGA containing material and

hexafluoroisopropanol for the PGA-containing material. One week to 12 weeks after tube implantation, the tissue response was minimal (minimal inflammatory response). A thin connective tissue capsule was found around the implant. Macrophages were lined adjacent to the TEC-plasticized L-PLA implants after the fourth day of implantation. However, only a few macrophages were observed adjacent to the implant at the third month of the implantation. The characteristic nerve regeneration pattern for all the implants was a well-vascularized cable of nerve fibers (encased by a connective tissue sheath) running parallel across the nerve gap. Four to 6 weeks after the initial transection, the regenerated nerve through the triethyl-citrate plasticized tube had a average of 1000 myelinated axons (40% of the proximal stump) across the gap. Nyilas et al. stressed that a critical factor for maintaining mechanical integrity (at least until the axonal regeneration is completed) is the control of the biodegradation/resorption of these tubes. They mentioned three main factors that can affect this process: the inflammatory response, the chemical structure, and the composition. They postulated that these bioresorbable materials have a low inflammatory response that is mainly due to the nature of these polymers (non-inmunogenic), their surface free energy (predominantly non-polar), and the low amount of trauma seen in applying the surgical procedure. Thus, they concluded that the principal factors to be used to adjust the useful life (*in vivo*) of

these bioresorbable tubes is through their chemical structure and composition. Some examples of the this were the stereochemical configuration (L or D,L-PLA), the use of low molecular plasticizer (in different amounts), and the use of high molecular weight plasticizer. In summary, they demonstrated that a well-organized nerve cable (comprising 40% of the untransected-nerve myelinated axons) is formed across a 5 mm gap through all the series of bioresorbable tubes used (see above) in about 3 to 6 weeks. From this fact, it can be assumed that the mechanical integrity of these bioresorbable tubes was maintained (at least for 3 to 6 weeks) which allowed nerve regeneration across this nerve gap.

Henry et al. (1985) made a study of 3 basic types of polyester tubes (with wall thickness of 0.12 to 0.25 mm, internal diameters [IDs] of 0.25 mm, 0.50 mm, 0.75 mm, and 0.86 mm, and length of 5 [majority] to 15 mm) to bridge mouse transected sciatic nerves with nerve gaps of 3 mm (majority) to 8 mm. These tubes mainly included two types of D,L-PLA (MW = 100,000) that had two types of plasticizers in amounts ranging from 2% to 10% for TEC and 5% for HLA/S (copoly [1,6-hexylene-(1,1)-L-lactate/succinate]), and 3:1 composite of PGA/PBS [polyglycolic acid/poly(2,3-butylene succinate)]. These polyester tubes were made in the same way as described in Nyilas et al. (1983). They evaluated the specimens at 1, 2, 3, and 24 months (ages of mice of 3, 4, 5, and 26 months old, respectively as estimated by the statement in the article that the animals

were at least 2 months old at the time of implantation) after the initial implantation. No nerve regeneration was observed in tubes with a 0.25 mm ID or across nerve gaps of 8 mm. In 100% of the 2 and 5% TEC-plasticized D,L-PLA tubes (7/7) and PGA/PBS tubes (2/2), there were regenerated nerves that crossed the nerve gaps. However, only 50% of the 10% TEC-plasticized D,L-PLA tubes (11/23) and 30% of the 5% HLA/S tubes (3/11) had regenerated nerves that crossed the nerve gaps. Multiple small fascicles with a thick epineurium were found in all regenerated nerves at the four evaluation times studied. These regenerated nerves had fewer large myelinated axons than normal. In the region proximal to the tubes, evidence of some degree of retrograde degeneration was found (large myelinated axons were somewhat lower in number than normal) in these regenerated nerves. One to 3 months after implantation, the tube walls were swelled and deformed with a concomitant reduction in the internal diameter (some tubes were occluded). At 1 month, the initial ID of the TEC-plasticized tubes (0.75 mm), HLA/S-plasticized tubes (0.5 mm to 0.86 mm) and PGA/PBS tubes shrank to about 74% to 82%, 70%, and 94% of the original ID, respectively. At 2 to 3 months, the initial ID of the 10% TEC-plasticized tubes was reduced to about 90% of its original value. However, the reduced ID of the 2% TEC tubes (evaluated at 1 month) did not change at 3 months. After 2 years, the 10% TEC-plasticized D,L-PLA tubes disappeared completely and only a fusi-

form swelling of the nerve was seen (the last evaluation periods were 1 and 3 months for the 2 to 5% TEC tubes and 1 month for the HLA/S and PGA/PBS tubes). Thirty-four percent of the tubes with ID of 0.5 mm or less exhibited successful nerve regeneration (which was defined as when a regenerated nerve crosses the nerve gap and myelinated fibers are seen in the nerve distal stump). However, as the initial tube ID increased, the regeneration success was better (tubes with 0.75 mm ID were about 75% successful). In addition, the number of myelinated axons across the nerve gap (midpoint) increased as the initial tube ID increased. At 1 to 3 months, the mean myelinated axon number ranged from 874 ± 640 (with tubes of 0.5 mm ID) to 2416 ± 39 (with tubes of 0.86 mm ID). However, the mean myelinated axon number in the normal sciatic nerve was 4050 ± 150. The mean axonal area (which was seen to increase with mouse age) for the regenerated nerve was about 50% (up to a maximum of 7.5 μm^2 at 2 years) of the normal axonal area (up to a maximum of 12.3 μm^2 at 2 years) at the different intervals of specimen evaluation (1, 2, 3, and 24 months after the initial implantation). Also, the mean myelin sheath width (which was seen to increase with mouse age) for the regenerated myelinated axon was about 50 to 75% (up to a maximum of 0.99 μm at 2 years) of the normal myelin sheath width (up to a maximum of 1.3 μm at 2 years) at the different intervals of specimen evaluation (1, 2, 3, and 24 months after the initial implantation). The

ratios of calculated axon diameter to myelin sheath width for the normal nerve and the regenerated nerve were similar. Finally, Henry et al. concluded that the critical factors in nerve regeneration across nerve guides are biodegradability and the internal diameter of the nerve guides. The more biodegradable and/or the smaller the internal diameter of the nerve guide tubes, the more distortion and occlusion is possible and the less likely a successful nerve regeneration is to occur. Apparently, the D,L-PLA tubes (5% TEC or less) with an initial ID of 0.75 mm have a greater probability (seven of seven examples) of guiding regenerated nerves across the nerve gaps with less distortion than the D,L-PLA 10% TEC tubes (eleven of twenty-three examples) with an initial ID of 0.5 to 0.75mm.

Madison et al. (1984) transected rat optic nerves and repaired these nerves (with no gap between the cut ends) using different types of D,L-PLA tubes with 2% TEC as plasticizer (1.5 mm in length, 0.75 mm ID, and 0.20 WT) in order to compare the vascularization in these tubes. The D,L-PLA tubes were fabricated as described in Nyilas et al., 1983. Three types of D,L-PLA tubes were used: empty-D,L-PLA tubes, D,L-PLA tubes + collagen + fibrinogen, and D,L-PLA tubes + collagen + fibrinogen + antibody to Thy-1. Thy-1 antigen is a cell marker (cell surface glycoprotein) localized to ganglion cells in the rodent retina. Antibodies to Thy-1 antigen stimulate the formation of retinal ganglion cells *in vitro*. At 4 weeks, the nerve guides induced little inflammatory response

and there was no appreciable degradation of these guides. Also, at the same time, a tissue cable (composed of fibroblasts, macrophages astrocytes, oligodendrocytes, Schwann cells, numerous unmyelinated axons and a few myelinated axons) was formed between the proximal and distal stumps of all transected nerves. However, the vascularization of the tissue cables in the tubes containing the proteins was greater than in the empty tubes. Finally, Madison et al. concluded that these empty bioresorbable tubes support new vascularization that is necessary for the nerve regeneration, and that the addition of proteins, particularly collagen and fibrinogen, increases the new vascularization.

Seckel et al. (1984) used rat sciatic nerves in an effort to study the nerve regeneration through biodegradable tubes and to investigate the role of the distal stump in this regenerative process. These tubes (D,L-PLA, molecular weight average of 100,000, using 10% by weight TEC plasticizer) were prepared by employing a dip-molding technique using acetone as solvent. Two groups of tubes were used in this work (10 mm and 20 mm in length, 2 mm ID, and 0.25 mm WT). Tubes of each group were interposed between the distal and proximal stumps of severed sciatic nerves, forming nerve gaps. In the 10 mm tube group, severed nerves were sutured into the tubes with no distal stump ("infinite nerve gap"), for 10 mm nerve gap, 5 mm nerve gap, and no nerve gap cases (0 mm). Also, in the 20 mm tube group, severed nerves were sutured into the tubes with

no distal stump ("infinite nerve gap"), for 20 mm nerve gap, 10 mm nerve gap, 5 mm nerve gap, and no nerve gap cases (0 mm). In the gross examination, on the sixth week, nerve strands were seen to have crossed the nerve gaps of 10 mm, 5 mm and 0 mm in both tube groups (10 mm and 20 mm tube groups). The D,L-PLA was transparent and brittle and was enclosed by thin connective tissue layer. By the third month, a well-defined centered nerve cable enclosed by a thin connective tissue sheath was formed. At the midportion of the regenerated nerve cable, the diameter of this cable was approximately one-half to two-thirds of the diameter of the proximal and distal portion (central tapering). At this time period, only a ghost (associated with a thin connective tissue, and easily broken upon removal) of the D,L-PLA tube was found and there was no neuroma or significant inflammation. Histologically, a well-vascularized regenerated nerve with fascicles of various sizes was found by the third month. The count for the myelinated axons at the center of the nerve gap (10 mm or less cases) was about 40% (5500) of that of the proximal stump. Functionally, by the third month, the rats were able to flex an extremity that had been surgically treated. However, by 3 months, evidence of nerve degeneration (disintegration of proximal and distal stumps) was observed when the nerve gap was greater than 10 mm, or with no distal stump. Finally, Seckel et al. concluded that a multifasciculated nerve (with minimal scar and inflammation) can be formed

across a gap (< 10 mm) through a bioresorbable D,L-PLA tube (biodegradable within 3 months), and that the distal stump exerts an important trophic effect on axons in the proximal stump if the nerve gap is 10 mm or less.

Da Silva et al. (1985) used mouse sciatic nerves to quantify motor and sensory nerve regeneration through D,L-PLA (MW was probably 20,000; source: Polysciences, Inc., Warrington, PA) tubes (2 percent TEC as plasticizer) which were fabricated by using a dip molding technique (Nyilas et al., 1983). The dimensions of the D,L-PLA tubes were 5-6 mm in length and 0.75 mm ID. These nerves were transected and PLA tubes were interposed between the distal and proximal stumps, forming a 4 to 5 mm gap. They evaluated the motor and sensory axonal regeneration by retrograde labeling of the dorsal root ganglia (sensory) and the ventral horn (motor) cell bodies of the sciatic nerve with HRP (horseradish peroxidase). To label these cell bodies, they transected the nerve again in the distal part of the repair site (3 mm beyond the nerve guide) and sealed the nerve into a polyethylene tube filled with HRP solution with one end of the tube sealed with petrolatum jelly. Three days after each retransection, the L_3-L_5 dorsal root ganglia attached to the sciatic nerve and the lumbar enlargement of the spinal cord were first removed, then sectioned, and subsequently reacted with tetramethyl benzidine. The HRP of those HRP-containing cell bodies (labeled dorsal root ganglia cell bodies and ventral horn cell bodies)

reacted with tetramethyl benzidine to produce a blue color which was used to visualize these labeled cell bodies. Two weeks after the initial transection, no nerve cable formation was observed and there were no labeled cell bodies. However, at 4 and 6 weeks, regenerated nerves bridged the nerve gaps across the nerve guides. Also, the number of myelinated axons did not change significantly from 4 weeks (1,550 ± 232 axons) to 6 weeks (1,491 ± 591 axons). However, from 4 to 6 weeks, the number of labeled dorsal root ganglia cell bodies (DRG) and ventral horn cell bodies (VH) increased from 385 ± 20 (50% of total VH) to 527 ± 19 (66% of total VH) for the VH and from 933 ± 50 (25% of total DRG) to 1361 ± 192 (33% of total DRG) for the DRG, respectively. Da Silva et al. suggested that the increase of number of labeled cell bodies from 4 to 6 weeks with no increase in the number of myelinated axons, can be interpreted as evidence of axonal branching in the early regenerative stages. Thus, the use of the number of myelinated axons in regenerated nerves may not be an accurate index of the success of nerve regeneration. Also, they concluded that this study validates electrophysiological evidence for a stronger regeneration of motor axons than sensory axons through nerve guides.

Madison et al. (1985) transected mouse sciatic nerves to study the effects of laminin in nerve regeneration across a 4 to 5 mm gap through D,L-PLA tubes with 2% TEC as plasticizer (MW was probably 20,000; source: Polysciences,

Inc., Warrington, PA). These tubes (5 to 6 mm in length and 0.75 mm ID) were fabricated as described in Nyilas et at. (1983). The transected nerves were interposed using empty PLA tubes, and tubes with 80% laminin-containing gel. Two weeks after the initial transection, the initial transected nerves were retransected 3 mm beyond the distal stump. This retransection was interposed with a polyethylene tube filled with HRP (horseradish peroxidase) to retrogradely label the parent cell bodies of the sciatic nerve (dorsal root ganglia and the ventral horn) to confirm axonal regeneration (if any). For the empty PLA tubes, there were no labeled cell bodies and no nerve cable formation. However, for the laminin filled PLA tubes, a well-vascularized nerve cable (unmyelinated axons, Schwann cells, and macrophages) was found in the middle of the tubes, and labeled cell bodies were found in the dorsal root ganglia (15 ± 4) and in the ventral horn (49 ± 19). Finally, Madison et al. concluded that laminin (in a nerve guide) has a direct stimulatory and enhancing effect on peripheral nerve generation of motor and sensory axons.

Madison et al. (1987) used mouse sciatic nerves to compare the axonal regeneration between the bioresorbable D,L-PLA tubes (MW = 110,000; source: Instrumentation Laboratories, Inc., Andover, Massachusett); 2% TEC as plasticizer; empty or filled with laminin gel) and the non-bioresorbable polyethylene tubes [PE] (empty or filled with laminin gel). The dimensions of both types of

tubes were 5 to 6 mm in length, 0.76 mm ID, and 0.46 mm WT. These biodegradable tubes were fabricated as described in Nyilas et al., 1983. These nerves were transected and the tubes interposed between the distal and proximal stumps, forming a 4 mm gap. They evaluated the axonal regeneration (after 2, 4, and 6 weeks following the initial transection) by labeling the dorsal root ganglia and the ventral horn cell bodies of the sciatic nerve with HRP, and by counting the number of myelinated axons (MA) in the regenerated nerves (at the midportion of the nerve gaps). Results similar to those reported by Da Silva et al. (1985) and Madison et al. (1985) were observed for the empty PLA tubes (at 2, 4 and 6 weeks) and the empty PLA and laminin-filled PLA tubes (at 2 weeks). However, for the laminin-PLA tubes, unexpectedly, the approximate number of labeled DRG (900 ± 100, 20% of control) and VH cell bodies (390± 20, 50% of control) were significatively fewer compared with these results of the empty-PLA tubes (DRG = 1400 ± 200, 30% of control, and VH = 540 ± 20, 60% of control) at 6 weeks (even though they increased in number with time). For the PE, the laminin had a enhancing and significant effect on the number of labeled DRG (1800 ± 300 [laminin] vs. 900 ± 250 [empty]) and MA (1420 ± 490 [laminin] vs. 220 ± 110 [empty]) seen after 2 weeks of the implantation. However, this effect decreased significatively at 4 and 6 weeks even though the number of labeled DRG and MA slightly increased in both PE groups. Also, at 6 weeks, the

number of labeled DRG and VH, and MA for the laminin-PE tubes was significatively greater compared with those for the laminin-PLA tubes. Madison et al. concluded that these tubes filled with laminin increased the initial rate (at 2 weeks) of axonal regeneration compared to the empty tubes. In addition, they indicated that the enhancing effect of laminin decreases (in the case of PE tubes) or even reverses (negative effect on PLA tubes) at later times. Also, they postulated that this negative effect on PLA tubes is mainly due to the possibility that laminin may accelerate the biodegradation of the tubes, causing swelling of these tubes thus reducing the luminal size (Henry et al., 1985) with a concomitant drop in axonal regeneration. Finally, they showed that the initial delay in the axonal outgrowth in the PLA empty tubes does not prevent the axonal outgrowth in later times.

3.2.2.2 Cellular method

A representative example of a nerve repair technique using the cellular method is the fascicular tubulization that separates the epifascicle and the intrafascicular layers by an artificial fascicle at the repair site. Thus, the fascicular tubulization avoids the possibility of invasion of fibroblasts from the epifascicle and facilitates the axonal regeneration and the re-establishment of the perineurial layer.

3.2.2.2.1 Non-biodegradable cuff

In the work discussed in this section, silicone rubber was the only material used to make a non-biodegradable cuff. This had a multiple lumen configuration.

Daniel (1991) used rat sciatic nerves to compare three nerve repairs: epifascicular suture and two types of silicone rubber nerve grafts (single-lumen cuff, SLC, and multiple-lumen cuff with 7 channels, MLC). The cuffs were interposed between the distal and proximal stumps of the transected nerve, forming a 5 mm gap. These cuffs were examined at different periods of time (8, 12, 16, and 24 weeks) after the initial transection. The electrophysiological analysis indicated nerve conduction in the regenerated nerve through the repair site; however, comparisons among the different nerve repairs were not performed. In the qualitative histological analysis, a minimal to moderate tissue reaction (with no neuroma) was observed in the SLC as well as in the MLC. Several nerve fiber bundles were formed in the MLC; individual nerve bundles filled each of the seven lumens. However, a single fascicle was found in the SLC and in the epifascicular suture repairs. In addition, the same patterns of axonal regeneration and nerve bundles were seen to cross the nerve gap into the distal stump in the MLC. In the quantitative histological analysis, the mean distal axon diameters, the total nerve cross-sectional areas, and the axonal cross-

sectional areas were not statistically different among the nerve repairs, but the mean axon diameters were smaller than those measured for the normal nerve control (5.7 ± 1.9 μm). Better functional analysis results were seen in the MLC compared to the other nerve repairs. Finally, Daniel concluded that this MLC can support, orient, and guide nerves regenerating through a 5 mm gap in the rat sciatic nerve with minimal to moderate tissue reaction.

3.2.2.2.2 Biodegradable cuff

In the studies discussed in this section, polyglycolic acid was the only material used to make biodegradable cuffs.

In 1983, Rosen et al. used rat peroneal nerves to compare two nerve repair techniques: fascicular suture and fascicular tubulization using PGA tubes. The PGA tubes were wrapped around the transected monofascicles, forming a 1 mm gap between the distal and the proximal stump of the monofascicles. Two to 26 weeks after the initial transection, the qualitative histological analysis revealed that the axonal organization was better in the fascicle tubulization (in general, good to excellent) compared to the fascicle suture technique (in general, fair), and the tissue reaction was minimal. However, at 49 weeks, the axonal organization was similar (good to excellent) in both repair types. The quantitative histological analysis results were similar in both nerve repair techniques (mean

axon diameter [about 4.5 μm], mean axon cross-sectional area [about 16 μm], and axonal count [2,500 to 3,000 axons]). Finally, Rosen et al. demonstrated that the fascicular tubulization technique improves the axonal organization in the regenerating nerve in comparison to the fascicular suture technique, but does not improve the nerve maturation.

In 1989, Marshall et al. used rat peroneal nerves to compare two nerve repair techniques: fascicular tubulization with a PGA-nerve coupler and a fascicular suture technique. The PGA-nerve coupler was composed of a central hollow housing (7 mm in length) that enclosed proximal and distal tubes (each one of 1.0 mm ID) that were used to guide the proximal and distal stumps of the transected nerve fascicle to the center of the nerve coupler (i.e., no gap between the stumps). The center area of the housing was 2.5 mm^2. Nine to 15 months after the initial transection, the axonal organization in the repair site was seen to be excellent in the PGA-nerve coupler, but ranged from fair to excellent for the fascicular suture technique repairs. The tissue reaction associated with the use of both techniques was minimal. For the quantitative histological analysis results, the mean distal axon diameter was seen to be slightly larger in the fascicular suture technique compared to the PGA-nerve coupler technique. The electrophysiological analysis did not show a statistical difference between the two techniques (both conduction fractions were approximately 58%). Finally,

Marshall et al. concluded that both techniques yield similar physiological results, that the axonal organization is better for the PGA-nerve coupler than for the suture technique, and that the surgical procedure in the PGA-nerve coupler is easier and quicker to perform compared to the fascicular suture technique.

In 1991, Hentz et al. used ulnar nerves and median nerves of primates to compare different nerve repair techniques: epifascicular suture, fascicular suture, and fascicular tubulization (1.0 to 1.5 mm between the nerve stumps) using PGA tubes. The different nerve repairs were examined at varying intervals after the time of repair. Seven months after the initial transection, the electrophysiological analysis demonstrated that these three different techniques had similar conduction fractions (about 81 percent). However, the epifascicular suture technique had a significantly longer mean added conduction delay (it is the added [to normal delay] delay in the conduction of the nerve action potential at the repair site due to the axonal branching at the proximal site of the nerve transection). The mean axon diameters (approximately 5.2 μm) and the axonal organizations (fair) were similar in the three techniques. Finally, Hentz et al. concluded that the fascicular tubulization with the PGA tubes promotes axonal regeneration that is as good as the fascicular suture technique.

3.3 Characteristics and properties of polylactic acid

3.3.1 Synthesis

Some of the methods used to synthesize polymers of lactic acid are polycondensation and ring opening polymerization. The polycondensation of lactic acid results in PLA of low molecular weights (1×10^4). To produce PLA of higher molecular weights, the lactic acid has to be converted first to a cyclic diester, lactide, by condensation. Then, by ring polymerization at 130°C in vacuum with stannous octoate (50-500 ppm) as a catalyst, these lactides are converted to PLA of high molecular weights. See Figure 3.4 for details of the synthesis of polylactic acid (Gilding and Reed, 1979; Kumar, 1987).

3.3.2 Physico-chemical properties

There are four possible optically distinct polymers of lactic acid. L-PLA and D-PLA are the stereoregular polymers; D,L-PLA is the racemic polymer that is obtained from a mixture of D-lactic acid and L-lactic acid; and meso-PLA can be obtained from D,L-lactide (infrequently used). D-PLA and L-PLA are semicrystalline materials, but D,L-PLA is an amorphous material. Because of this difference in crystallinity, the L-PLA is usually used where high mechanical strength and toughness are needed (sutures and orthopedic devices). Conversely, D,L-PLA is usually employed in applications such as drug delivery, where there

is a uniform dispersion of the active species within a monophasic matrix (Engelberg and Kohn, 1991), and as biodegradable nerve regeneration cuffs (Nyilas et al., 1983; Madison et al., 1984, 1985, 1987).

The density for the D,L-PLA (MW = 20,000) is approximately 1.241 ± 0.018 (measured in our laboratory). L-PLA (MW = 50,000 to 300,000) has a melting point (T_m) of 170 ± 10°C. The low T_ms are for the L-PLA species with low MWs and crystallinities. However, the D,L-PLA has an indefinite T_m. The glass transition temperature (T_g) for the D,L-PLA (MW = 20,000 to 550,000) and L-PLA (MW = 50,000 to 300,000) is about 55 ± 5°C. As in the case of T_m, the lower

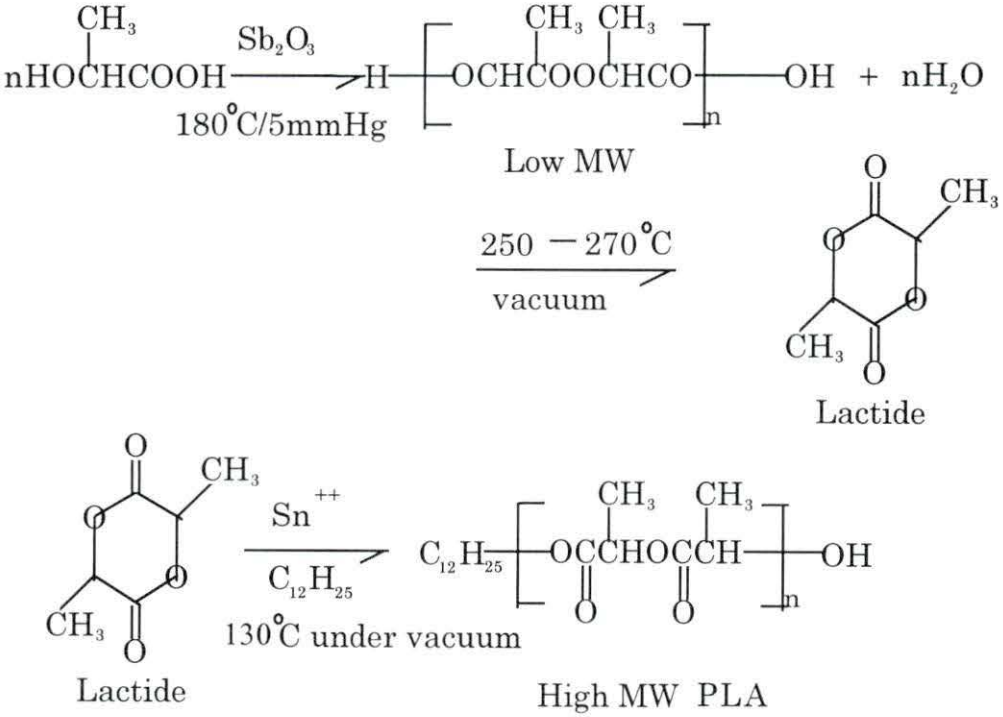

Figure 3.4: Synthesis of polylactic acid (Gilding and Reed, 1979; Kumar, 1987)

T_g is for the PLA species with lower MW and crystallinities. The temperature of decomposition for these PLA species is about 249 ± 8°C. Some of the decomposition products that can be generated at this temperature are carbon oxides (material safety data sheet from Polysciences, Inc., Warrington, PA, 4/25/94). Also, some of the characteristics (such as initial MWs and optical activity) of PLA are affected by the processing of the initial material. In all varieties of PLA, the initial molecular weights are reduced significatively after compression or injection molding. In addition, semicrystalline PLA can change to amorphous PLA after sudden cooling from the melted material (Engelberg and Kohn, 1991; Gogolewski et al., 1993).

L-PLA (MW = 50,000 to 300,000) has better mechanical properties (tensile strength [TS], tensile modulus [TM] and flexural storage modulus [FSM, bending modulus of elasticity]) than the D,L-PLA (MW = 20,000 to 550,000) for respective MW comparisons. Furthermore, high-MW L-PLA (MW = 300,000) is one of the strongest biodegradable medical polymers in terms of TS, TM and FSM (48, 3,000 and 3,250 MP_a, respectively). One of the drawbacks of PLA (MW = 20,000 to 550,000) is its notable brittleness (fracture elongation [FE] = 2 to 6 %). Here, the D,L-PLA is more ductile (compared with L-PLA) with a significatively larger proportion of plastic deformation than elastic deformation in fracture elongation (FE = 5 to 6 %). Some of the differences in mechanical proper-

ties can be due to difference in crystallinities. Refer to Table 3.1 for a summary of selected properties of PLA (Engelberg and Kohn, 1991; Schindler et al., 1977).

3.3.3 Biodegradability and biocompatibility

Biodegradability and biocompatibility are important properties of biodegradable medical implants. It is important to know how the biodegradable material reacts in the physiological environment of the animal or human body (material biodegradation characteristics) and how the host responds to the presence of the material (tissue response) to consider and apply this knowledge to the appropriate use of the material *in vivo* in a particular application. In the next sections, biodegradability and biocompatibility of PLA will be discussed.

3.3.3.1 Biodegradability

There are four stages of *in vivo* polymer biodegradability. The first is the hydration stage in which there is disruption of Van der Waals forces and hydrogen bonds. The degree, rate and effect of this hydration process are dependent upon the hydrophilic nature of the implanted polymer. Polyesters absorb relatively little water in comparison with natural polymers and hydrogels (where there is a substantial reduction in mechanical strength). The second stage is the biodegradation stage which involves the cleavage of the polymer backbone, and as consequence of this, a loss of strength. In biodegradable polyesters, the main

Table 3.1: Summary of selected properties of polylactic acids (Engelberg and Kohn, 1991; Schindler et al., 1977)

Polylactic acids	Supplier	M_w[a]	Characterization			Thermal analysis			Crystallinity %	Mechanical properties					Solubility
			M_w[b]	M_n[b]	η[c]	T_d (°C)	T_m (°C)	T_g (°C)		TS MPa	TM MPa	FSM MPa	Elongation Yield %	Elongation Break %	
L-PLA	Polysciences Inc.[d]	50,000	64,800	19,600	0.61	242	170	54	30	28	1,200	1,400	3.7	6.0	methylene chloride, chloroform
L-PLA	Polysciences Inc.	100,000	139,000	43,200	1.65	235	159	58	15	50	2,700	3,000	2.6	3.3	same as above
L-PLA	Polysciences Inc.	300,000	375,000	150,000	3.08	255	178	59	29	48	3,000	3,250	1.8	2.0	same as above
D,L-PLA	Polysciences Inc.	21,000	16,500	13,400	0.25	255	/e	50	amorphous	/e	/e	/e	/e	/e	acetone, benzene
D,L-PLA	Stolle R&D Corp.	107,000	98,500	66,300	0.64	254	/e	51	amorphous	29	1,900	1,950	4.0	6.0	same as above
D,L-PLA	Stolle R&D Corp.	550,000	410,500	163,500	2.01	255	/e	53	amorphous	35	2,400	2,350	3.5	5.0	same as above

[a]Absolute weight average molecular weights as provided by the suppliers.
[b]Weight average molecular weight (M_w) and number average molecular weight (M_n) determined by gel permeation chromatography in chloroform relative to polystyrene standards.
[c]Intrinsic viscosity determined in chloroform at 30 °C. Intrinsic viscosity (limiting viscosity number) is in dL/g.
[d]Warrington, PA
[e]Not available

mechanism for the chain scission is by simple hydrolysis of the ester bonds. In addition, the chain scission rate in these polymers is especially dependent upon the degree of the crystallinity (the higher crystallinity, the lower the biodegradation rate). In the case of semicrystalline polymers, the chain scission occurs first in the amorphous regions. The third stage is the bioerosion stage. Here, there is a further cleavage of the covalent bonds until the polymer is degraded to a low molecular weight level in which physical and mechanical integrity are compromised and the initial loss of mass occurs. The actual molecular weight level is dependent on the T_g and crystallinity, among other contributing factors. The fourth stage is the bioassimilation stage. In this stage, the resultant polymer fragments are solubilized, phagocytized and ultimately (for the truly biodegradable polymer) metabolized (Kronenthal, 1975; Kumar, 1987). The time required for the complete biodegradation of these polymers depends of the degree of crystallinity, T_g, and initial molecular weight (Dijkstra et al., 1990).

In relation to PLA, the degradation rate is mainly influenced by optical activity and the presence of additives such as plasticizers or impurities (Nyilas et al., 1983). The TEC plasticizer accelerates the biodegradation of PLA due to an increase in chain mobility of these polymers. If the concentration of the plasticizers is increased, the time for biodegradation to occur is decreased even more. Thus, the initial loss of weight and the beginning of loss of mechanical

integrity for the plasticized polymer would occur in less time than the expected for the unplasticized polymer (lesser time with increased concentration of the plasticizer). One way to reduce this accelerating effect and to prolong the duration at which mechanical integrity loss begins is by increasing the molecular weight of the plasticizer. This would reduce the diffusion rate of the plasticizer to the tissue, and that would diminish the accelerating effect of the plasticizer on biodegradation. The autocatalyzed chain scission reaction of these polyesters (catalyzed by the degradation products, carboxylic acids) is described by the following first order equation: $\ln(M_n) = \ln(M^{\circ}_n) - kt$ [M°_n = initial M_n, ln = natural logarithm base *e*, k = rate constant, t = time]. The D,L-PLA varieties have a higher average rate constant of 5×10^{-2} day^{-1} compared to 2.3×10^{-3} day^{-1} for the L-PLA. This difference is mainly due to the partial crystallinity of the L-PLA (Dijkstra et al., 1990).

It is postulated in the literature (Gogolewski et al., 1993; Therin et al., 1992) that the degradation process progresses quicker in the center of the material (PLA) than at the surface. Here, the degradation products (carboxylic acids) are accumulating in the central part of the material because of the slow diffusion of the products through the mass of the polymer. Thus, the degradation is faster in the core of the material because of the increased autocatalytic effect of these carboxylic acids. Then, as a consequence of this heterogeneous process, a

hollow structure can eventually be formed. This heterogeneity in the degradation is more pronounced in injection and compression molded materials (Gogolewski et al., 1993). In the injection and compression molded process, a greater molecular orientation is usually observed in the surface of the molded materials than in the inner part where there is practically no orientation.

In biodegradation studies with D,L-PLA films (dimensions: 20 mm x 10 mm and thicknesses of 0.13 mm to 0.85 mm; with a M_n of 14,000) that were subcutaneously implanted in rabbits, approximately 11% of the initial mass and 33% of the initial M_n were lost as measured for samples retrieved 4 to 5 weeks after the initial implantation (Pitt et al., 1981; Schindler et al., 1977). Also, these films lost about 25% and 100% of their initial mass (or 66% and more than 90% of the initial M_n) after 12 and 28 weeks of the implantation. When the M_n of these films was increased, the loss of the initial mass occurred at a later time. D,L-PLA films with a M_n of 49,000 began to lose mass after 20 weeks of the implantation (M_n decreased 70% to a level of 15,000). These films lost between 25% and 100% of their initial mass (or more than 90% of the initial M_n) after approximately 32 and 60 weeks of implantation. When the M_n of these films was increased to 112,000 and 185,000, the initial loss of mass occurred about 34 and 42 weeks after the implantation (M_n decreased to 12,000 and 15,000). For these films, more than 50% (or more than 95% of the initial M_n)

and probably 100% of the initial mass were lost after 12 and 18 months of the implantation. In summary, after six months of implantation, the weight loss percentages for these D,L-PLA films were 0%, 15%, and 100% with initial M_n of 100,000 or greater, 49,000, and 14,000, respectively. Also, at this time, the reduction percentage of the initial M_n of these films varied from about 80 to 90%.

On the other hand, other studies have indicated that after 6 months of subcutaneous implantation in mice, L-PLA discs (dimensions: diameter = 15 mm and thickness = 2 mm; M_n from 85,300 to 5,200 or M_w from 275,000 to 34,000) had less mass and less M_n reduction (0 to 10% of the original mass or about 70 to 80% of the initial M_n) compared with D,L-PLA of similar M_n (Gogolewski et al., 1993). In addition, Pistner et al. (1993 a, b) showed that L-PLA blocks (3 x 3 x 2 mm) with a M_n of 160,000 (M_w = 450,000) are completely gone after subcutaneous implantation in rats for 2 years. The route of elimination for PLA is probably through the lungs as carbon dioxide and water (Gilding, 1981; Kronenthal, 1975).

3.3.3.2 Biocompatibility

Biocompatibility of a material can be defined as the capacity of this material to perform a specific function in a determined tissue or organ with an appropriate host response in a particular application. Also, this material has to be

non-toxic, non-immunogenic, non-carcinogenic, and non-thrombogenic (Williams, 1989; Vert, 1990). In case of biodegradable polymers, the degradation products should primarily be natural metabolites (e.g., lactic acid from PLA) that can dissolve in the extracellular fluid or be easily phagocytized (commonly, by macrophages), and subsequently excreted through the lungs as CO_2 and H_2O. However, this material can sometimes fragment into large pieces, and multinucleated giant cells can be formed to remove these pieces. The typical tissue response to a film sample of a biocompatible biodegradable polymer is the formation of a thin fibrous capsule around the implant, with a lining of macrophages ingesting the breakdown products until mass loss is complete (at which time the capsule and macrophages disappear). This mass loss should be completed within 6 months to decrease the possibility of the biodegradable implant inducing carcinogenesis (Gilding, 1981). This is observed particularly in mice and rats and is independent of the nature of the implant. However, chronic inflammation can inhibit the tumor formation (Pistner et al., 1993 a, b).

In relation to PLA, no matter the site of the implantation or the configuration, these polymers exhibit good biocompatibility. Also, there have been no significant adverse tissue reactions observed in animals and humans for PLA polymer implants that have traces of initiators of polymerization, ethylene ox-

ide, or solvents such as acetone, methanol, methylene chloride or dioxane (Gogolewski et al., 1993).

In addition, Gogolewski et al. (1993) reported that when discs of this material (2 mm in thickness and 15 mm in diameter, M_w from 33,000 to 275,000 or M_n from 5,200 to 83,500) were implanted subcutaneously in mice, no acute inflammation, abcess formation, or tissue necrosis was detected around the discs (nor was there tissue reaction distant from the implant). The fibrous capsules that were formed around the discs decreased in thickness (from 100 μm after 1 month of implantation to 60 μm after 6 months of implantation) and cellularity (with fibrocytes, macrophages, lymphocytes, foreign body cells, and mast cells after 1 month of the implantation changing to a few sporadic fibrocytes and macrophages, but with the same number of mast cells after 6 months of implantation) with increasing time.

4. MATERIALS AND METHODS

4.1 Design and fabrication of the biodegradable nerve regeneration cuff

4.1.1 General

For the development of biodegradable nerve cuff, there are least four considerations that have to be taken into account: chemical and structural, biological, design and fabrication considerations. The chemical and structural and the biological considerations of PLA have been discussed in previous sections. Some investigators that have used biodegradable material for fabrication of nerve regeneration cuffs have chosen PLA [Nyilas (1983); Madison et al. (1984, 1985, 1987); Seckel et al. (1984); Da Silva (1985); Henry (1985)] because this material is very biocompatible and the products of biodegradation are metabolized readily by the human or animal body. The most interesting results of these studies are the low inflamatory response to the PLA cuffs and the biodegradation of this material that occurs in less than one year (specifically for the D,L-PLA variety [Seckel et al. 1984]). However, L-PLA varieties are more resistant to biodegradation (up to 2 years) and more prone to induce carcinogenesis (Gilding [1981]). This induced carcinogenesis is particularly observed in mice and rats and is in-

dependent of the nature of implant [Pistner et al., 1993 b] (the biodegradation should be completed within 6 months to decrease that possibility [Gilding 1981]). Therefore, the D,L-PLA variety was chosen for making the proposed biodegradable nerve cuff.

4.1.2 Design of the biodegradable nerve regeneration cuff

Considering recent research with respect to the improvement of mechanical support, guiding and orientation of regenerated axons across a nerve gap, a seven-lumen cuff (7LC) design was chosen for the fabrication of a biodegradable nerve guide (D,L-PLA). The dimensions and arrangement of the nerve cuff of the present study were similar to the multiple-lumen cuff used in Daniel, 1991. These cuffs had a outer diameter of 3.35 mm. The projecting ends of these 7LC (where the ends of a transected nerve would be inserted and sutured) had a length of 2 to 4 mm, a inner diameter of 2.45 mm that is slightly larger than the actual diameters of rat sciatic nerves at mid-thigh level (1.2 to 1.6 mm; Daniel, 1991), and a wall thickness of 0.45 mm. The length chosen for the central part of the 7LC (with the 7 holes, hole diameter. = 0.33 mm) was 10 mm because this is the maximum distance (on rat sciatic transected nerves) that the distal stump exerts an important trophic effect on axons in the proximal stump, and as a consequence, regenerated nerves can be bridged across that distance (Seckel et

al., 1984). The total length of this 7LC was 14 to 16 mm. A longitudinal section through the middle of the seven-lumen cuff is shown in Figure 4.1.

The 7LC had the seven holes, six of which were arranged in a hexagonal pattern around a central hole. The distance between the inner diameter of the projecting ends and the external holes was approximately 0.39 mm. Also, the distance between the central hole and the external holes was approximately 0.35 mm (see Figure 4.2).

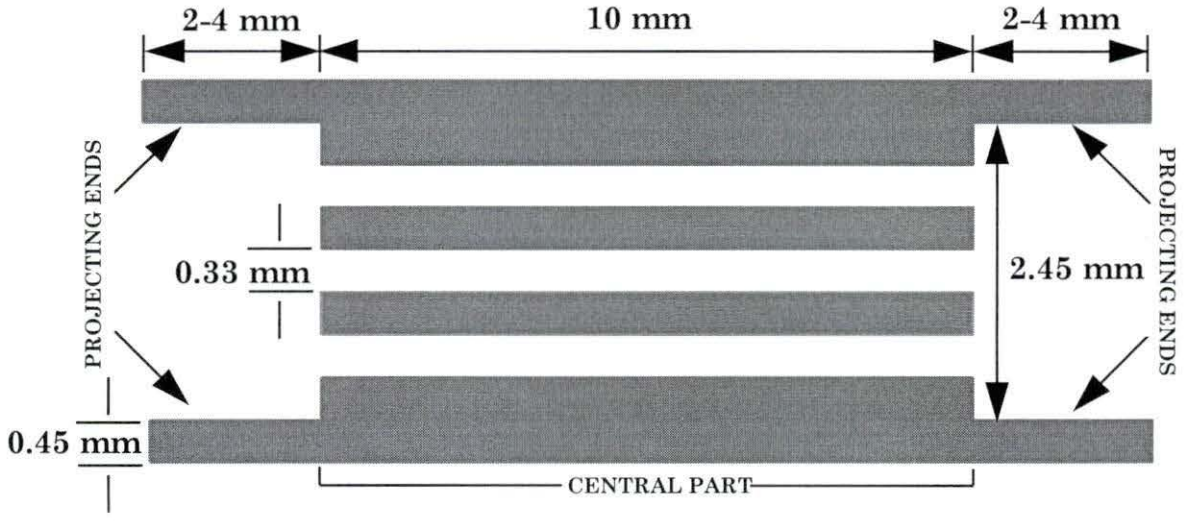

Figure 4.1: Longitudinal section through the middle of the seven-lumen cuff

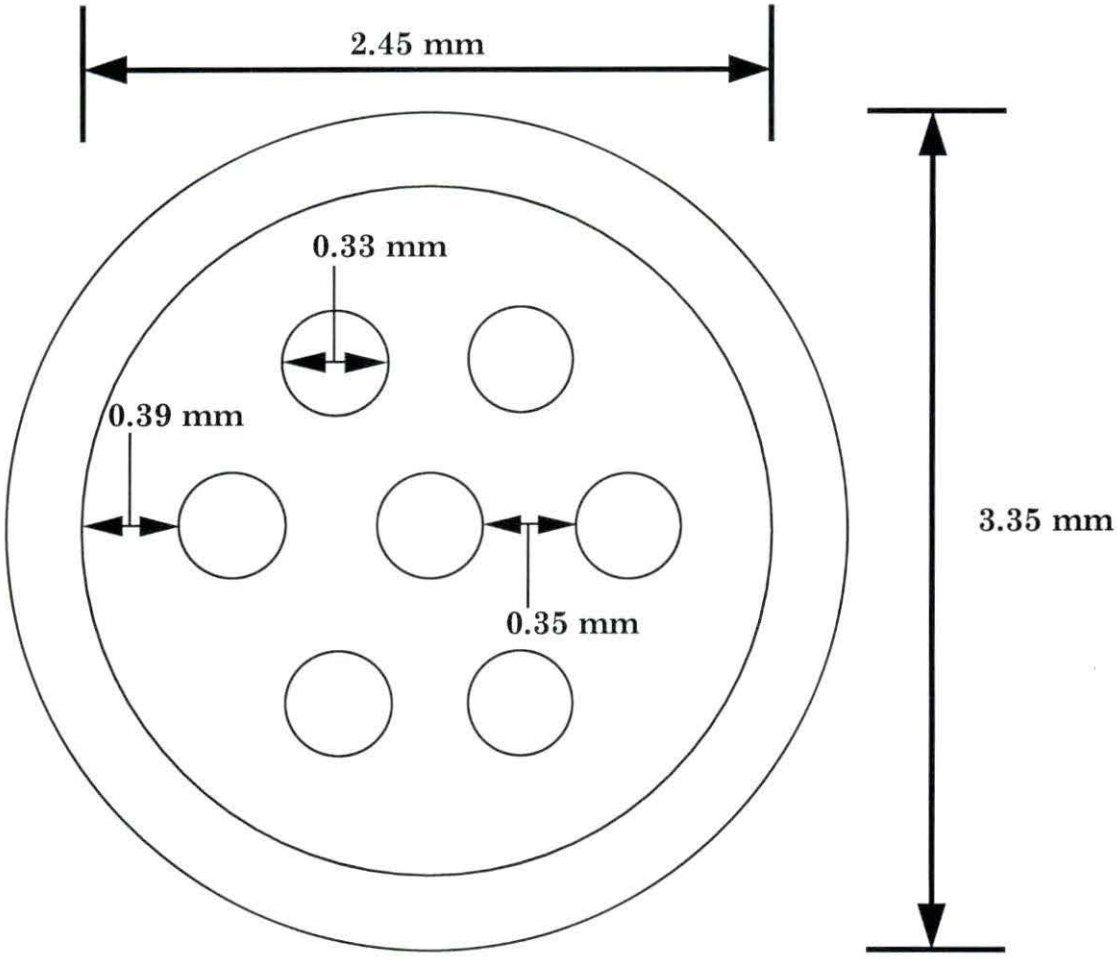

Figure 4.2: Cross section through the 7-lumen cuff and the hexagonal lumen pattern around a central hole

4.1.3 Fabrication of the biodegradable nerve regeneration cuff

For the fabrication of the 7LC, an oven (Isotemp^R vacuum oven, model, 282 A) was used to heat the D,L-PLA material in the mold (see below for details) at 205 °C. The temperatures of the melted material were taken from digital output of the oven used and by a digital multimeter (Fluke, model 8024B). The total time that the material was heated was about 4 hours. The resultant melted material was cooled in air for five to ten minutes. The resultant parts, central and outer parts (projecting ends in Figure 4.1), were glued with acetone to form the 7LC assembly (see next section for details).

4.1.3.1 Mold setup

The seven-lumen cuff was made from D,L-PLA with a weight-average molecular weight of 20,000 (Polyscience, Inc., Warrington, PA) and an estimated a number-average molecular weight of 13,400 (Engelberg and Kohn, 1991). It was made in two parts: the outer parts (the two projecting ends of the cuff) and the central part (where the seven holes are located), see Figure 4.1. Two similar mold systems were needed to make these cuff parts. Both molds were held in a vertical position by a glass tube (100 mm in length for the cuff central part or 70 mm for the cuff outer parts, 7 mm OD, and 4.95 mm ID) that was inserted in a hole in an aluminum plate (hole was 7 mm in diameter in the first 5.35 mm of

depth and 3.18 mm in diameter in the last 1 mm of depth; the plate had a thickness of 6.35 mm).

For the first steps of the melting process procedure (see experimental setup for details), these glass tubes were inserted into an aluminum tube (60 mm in length, 25 mm OD and with three internal holes of 7 mm in diameter [triagularly arranged with a length of about 58 mm]). The outer part of both molds consisted of a silicone rubber (SR #1) tubing (3.35 mm ID x 4.65 mm OD, and 125 mm in length for the central cuff part or 95 mm for the outer cuff parts). For the mold system of the outer cuff parts, 5 mm of the bottom part of the SR #1 was sealed with a silicone rubber (SR #6) tubing (Dow Corning, Medical Grade Tubing = 1.02 mm ID x 2.16 mm OD, and 5 mm in length) that had inside it a press fit capillary tube (CP #2, 1.02 mm ID x 1.40 OD, and 5 mm in length). The CP #2 expanded the SR #6 tubing to fill the 3.35 mm diameter spacing of the SR #1 tubing. The upper end (which was in contact with melted material) of the SR #6 tubing and CP #2 tube assembly was sealed with Silastic^{R} Medical Adhesive (Dow Corning). The cure time for this silicone was about 24 hours in air. Also, for this mold, an external modified capillary tube (external modified CP #1) was used to make these outer parts in the melting process (see the next section). This capillary tube (CP #1, 100 mm in length, 1.50 mm ID, 2.16 mm OD) that was sealed at the lower end with Silicone Type A was covered

by two silicone rubber tubings (SR #4, 1.40 mm ID x 1.96 mm OD x 100 mm in length, and SR #5, 1.57 mm ID x 2.41 mm OD x 110 mm in length, Dow Corning, Medical Grade Tubing). Here, the SR #4 tubing was expanded and press fitted into the CP #1 tube. Subsequently, the SR #5 tubing was expanded and press fitted into the SR #4-CP #1 compound tube, forming the external modified capillary tube (external modified CP #1). The bottom part of this capillary tube (CP #1) was covered only by the SR #4 tubing. This covered bottom part had a final OD of 2.46 mm. The upper part of this capillary tube (CP #1) that was covered by the SR #4 and SR #5 tubings had a final OD of 3.25 mm. From the upper end of this capillary, a 20 mm extension of the SR #5 protruded. For the mold system of the central cuff part, a modified 7-lumen silicone rubber (SR #2) tubing (original tubing used in Daniel, 1991) was made. The SR #2 tubing was prepared by cutting the ellipsoid excess of the original 7-lumen silicone rubber tubing with a industrial razor (single edge), obtaining a shaved tubing with a average diameter of 2.11 mm. Then, this shaved tubing was press fitted into a silicone rubber (SR #3) tube (Dow Corning, Medical Grade Tubing, 1.57 mm ID x 2.41 mm OD, and 10 mm in length). The final dimensions of the SR #2 were the following: 10 mm in length, 3.35 mm in diameter, and 7 holes with the same hexagonal arrangement of six holes around a central hole and the approximated dimensions seen in Figure 4.1 (central part) and Figure 4.2. Seven plain carbon

steel pins (covered with a thin film of silicone rubber cured for 24 hours [less than 0.01 mm in thickness], 0.33 mm ID, and 30 mm in length) were press fit into the 7 holes of the SR #2 tubing. To cover these steel pins with silicone, a solution of 1:10 [weight (grams)/volume (cubic centimeters)] of Silastic^{R} Medical Adhesive Silicone Type A to hexane was prepared. Then, the pins were slowly immersed in vertical position into this solution 3 times, waiting between each immersion and after the last coating about 10 to 15 seconds. Then, this SR #2 tubing with the steel pins was press fitted into the bottom part of the SR #1 to make the mold system to fabricate the central part of D,L-PLA 7-lumen cuff. Fourteen millimeters length of these pins were inside the SR #1 tubing. The upper part (3 to 4 mm) of these pins was held together by inserting 3 to 4 mm of the original 7-lumen tubing, then maintaining this 7-lumen insert parallel and straight to these seven steel pins. This particular original tubing insert was shaved (after it was inserted), and the external silicone material trimmed (just beyond the external part of the 7 pins). See Figure 4.3 and Figure 4.4 for the diagrams of the mold systems needed to make the D,L-PLA 7-lumen outer and central parts, respectively. In the next section, the experimental procedure to make these two parts will be discussed.

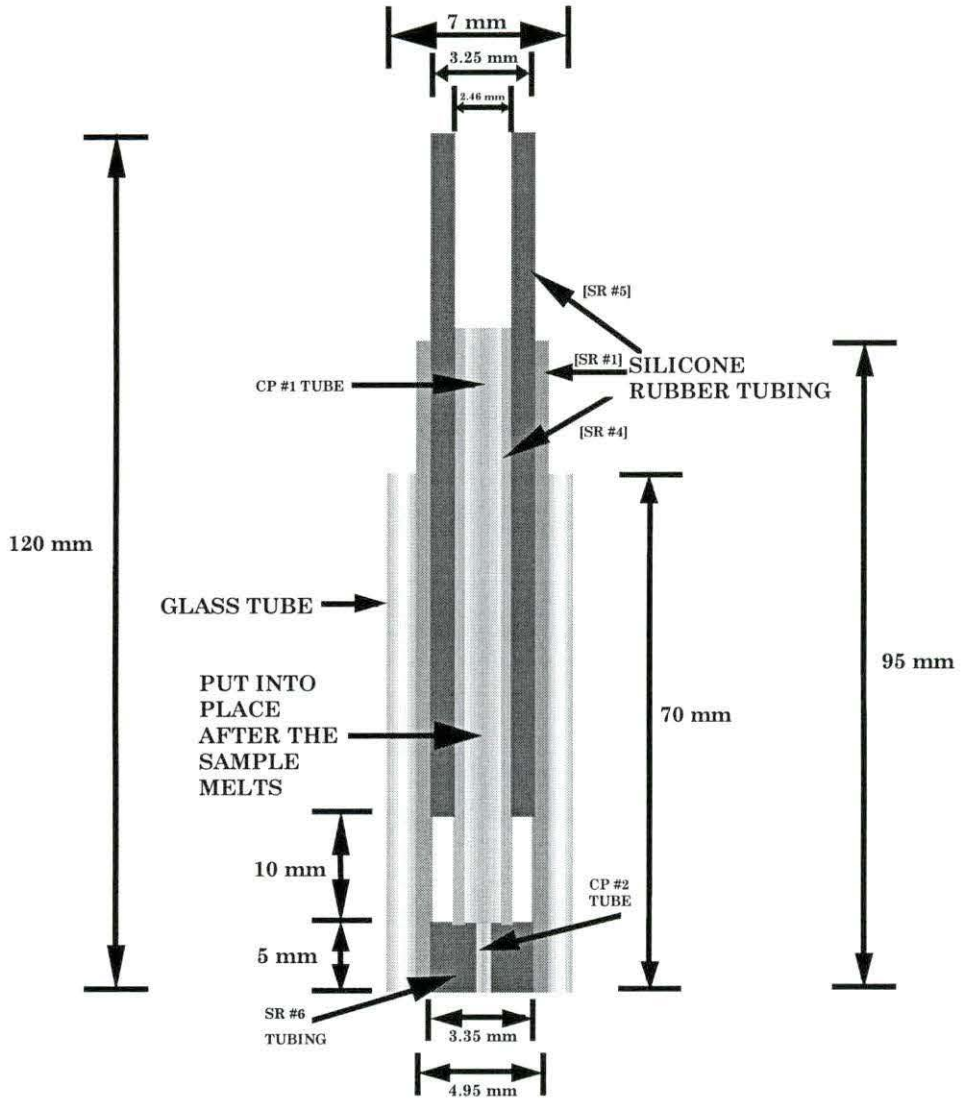

Figure 4.3: Diagram for the mold system used to make the 7-lumen cuff outer parts (not to scale)

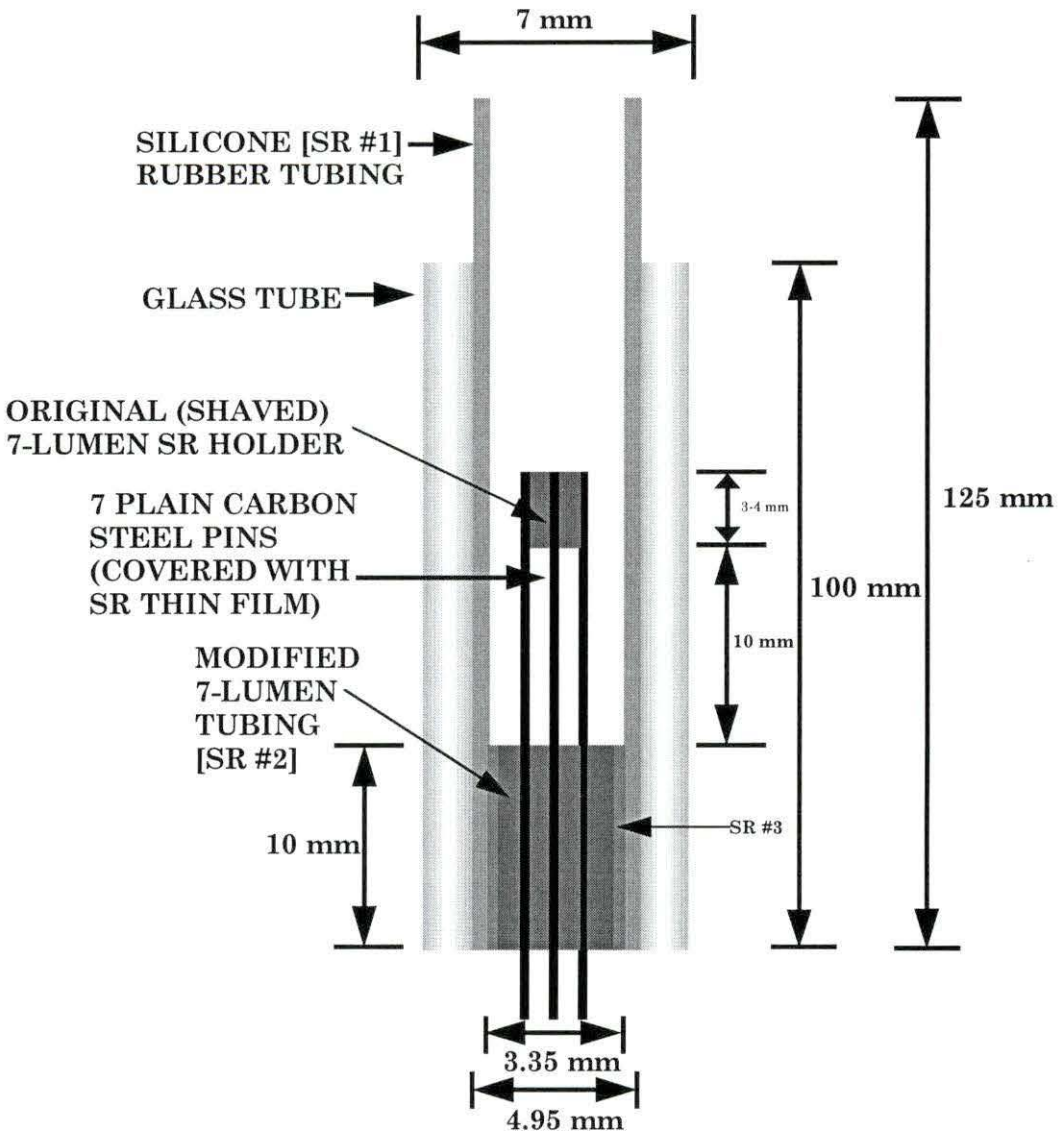

Figure 4.4: Diagram for the mold system used to make the 7-lumen cuff central part (not to scale)

4.1.3.2 Experimental setup

Two different procedures were undertaken to make the central and the outer cuff parts (one for each part type). Details for each of these are discussed in the following sections.

4.1.3.2.1 Central cuff component procedure

All of the mold parts were cleansed with a mild Snow White^R detergent and rinsed profusely with deionized water. After that, they were dried in an oven [150- 200 °C] for 15-20 minutes. The steps to make the central part of the D,L-PLA 7-lumen cuff were the following:

1. 140 mg of D,L-PLA (MW = 20,000, see above) was put in the mold system (Figure 4.4), allowing that sample (particles of a flake-like form) to compact over the upper part of the steel pins.
2. Then, the mold was put into a preheated oven at 205 °C. The mold was placed into the aluminum mount (preheated to a temperature of 190 - 195°C in the oven, measured by a digital multimeter, Fluke^R model 8024) for at least 3 hours to achieve a stable temperature of 190 to 195 °C. The aluminum mount (refer to the previous section) held the mold straight.

3. After 3 hours in this aluminum mount, the mold was then placed into a hole in the preheated aluminum plate (at 205 °C, see last section) to complete the melting of the PLA sample around the 7 steel pins. The PLA melted material was seen through the glass tube of the mold.
4. After the sample was without apparent bubbles (about 4-5 hours of the initial heating), the mold and the sample were cooled to room temperature. It took about 10 minutes to reach room temperature (about 25-30 °C).
5. Then, the 7 steel pins were manually removed using a metal gripper. With the help of an industrial razor (single edge), the wall of the outer silicone rubber [SR #1] tubing was then cut longitudinally and opened. Then, the resultant central part with the 7 holes was taken from [SR #1] tubing. Then, with an industrial razor (single edge), both ends of the resultant central part were trimmed to obtain a flat surface. The holes were cleaned by inserting clean mercerized cotton covered polyester threads (about 50 cm in length and 0.25 mm ID) into the holes (sliding the threads only one time [from back to front] against all the surfaces of the holes). Care was taken to avoid much pressure and much deformation over the hole surfaces.

4.1.3.2.2 Outer cuff procedure

All of the mold parts were cleansed with a mild Snow White^R detergent and rinsed profusely with deionized water. After that, they were dried in an oven [150- 200 °C] for 15-20 minutes. For making the outer parts of the D,L-PLA 7-lumen cuff the procedure was the following:

1. About 100 mg of D,L-PLA (MW = 20,000, see above) was put in the mold system (Figure 4.3), allowing that sample (particles of a flake-like form) to compact over the upper part of the SR #6 tubing.
2. Then, the mold was put into a preheated oven at 205 °C. The mold was placed into the aluminum mount (preheated to a temperature of 190 - 195°C in the oven, measured by a digital multimeter, Fluke^R model 8024) for at least 3 hours to achieve a stable temperature of 190 to 195 °C. The aluminum mount (refer to the previous section) held the mold straight.
3. After 2-3 hours in this aluminum tube, the mold was put in a pre-heated aluminum plate (at 205 °C, see last section) to complete the melting of the sample. The PLA melted material was seen through the glass tube of the mold.
4. After the sample had no apparent bubbles (about 3-4 hours of the initial heating), the bottom part (about 10 mm) of the modified glass

capillary (CP #1) tube (see last section) was slowly immersed into the melted sample (taking care that no bubbles were formed). Then, the mold and the sample were cooled to room temperature. It took about 10 minutes to reach room temperature (about 25-30 °C).

5. With the help of an industrial razor (single edge), the wall of the outer silicone rubber [SR #1] tubing was then cut longitudinally and opened. Then, the resultant tube was taken from the outer silicone rubber tubing and pulled from the modified glass capillary. Then, this tube was cut, with the razor blade, to obtain 2 tubes or outer parts.

The resultant central and two outer parts were glued together to make the 7LC assembly. Acetone was used as the solvent. Both parts were wetted using a little clean brush (the central part was wetted just beyond the holes). Then, these parts were joined together, taking care that both parts were aligned. The resultant 7-lumen cuff was left at room temperature for 1 to 2 days. The cuff was then stored in a desiccator prior to performing characterization measurements for the 7LC assembly.

4.2 Characterization of the biodegradable nerve regeneration cuff

The assembly of the two outer and one central part was examined visually and microscopically. For microscopic examination, the 7LC was positioned over a platform (white background) and observed using a stereo microscope (Nikon^R

98660, Japan) at 30 X. Also, the holes of the central parts were examined microscopically. Here, it was possible to examine (by varying the focus) about the first 3-4 mm of each end of the central part.

Also, weight and dimensional measurements of both the central and outer parts were made. For weight measurements, a Mettler^{R} balance was used (model H31AR/H311). For dimensional measurements, a dial caliper (wrench style, stainless steel hardened, with 0.001 inch unit division) and a linear micrometer (inserted in one ocular lens (10 X) of the stereo microscope and with a 0.001 inch unit division at 30 X [total magnification]) were used. Densities were calculated for the central parts taking into account the absence of material associated with the 7 internal holes in the calculation. The following is an example of the density calculation (L = length of the central part, OD = outer diameter of the central part, HD = internal hole diameter of the central part, and G = weight of the central part):

$$\text{density} = \frac{4G}{\pi L \left[(OD)^2 - 7(HD)^2\right]}$$

5. RESULTS AND DISCUSSION

5.1 Results

The resultant central part and outer parts of the cuffs were free of micro-bubbles (characterized to a size as small as 2 μm in diameter), translucent, and with a very light amber color when examined visually and microscopically (30 X). Also, no inhomogeneities were observed through the assembly of parts. However, sometimes, few small black particles (4 to 8 particles of approximately 20 to 50 μm in diameter) were seen throughout the assembly parts. These parts were hard but somewhat ductile. When sectioning into parts, the slices did not break apart. In addition, when the outer parts were pierced manually with needle to provide suture anchor points, they yielded with little pressure, but the outer surface cracked. The external surfaces of these two parts, the internal surfaces of the outer parts and the internal holes of the central part, appeared smooth at 30 X. However, after the plain carbon steel pins were pulled from the central parts (see last section), some particles were seen mainly at the ends of these parts. Most of these particles (maybe silicone rubber residues from the plain carbon steel pins or steel particles from these pins) were removed after tedious cleaning using the mercerized cotton covered polyester threads (see last

section). For the cuff assembly, the outer part adhered very well to the central part by using acetone as the gluing agent. The region where both parts were joined was firm. However, a few microbubbles (approximately 12 to 16 bubbles from 50 to 250 μm [average = 76 ± 25 μm] in diameter) were observed in that region. Probably, these few microbubbles were produced because these two parts were not completely flat since the surfaces had some imperfections produced by the cutting of the surface using the razor blade. These microbubbles appeared to be mainly in the outer surface of the joint of the outer and central cuff parts. Also, it was noted that sometimes slight misalignment of the internal holes had occurred in association with the molding procedure (especially at one end, where the metal pins were held at their upper part, see Figure 4.4). Figure 5.1 shows the resultant central part, outer parts, and the completed D,L-PLA 7-lumen cuff assembly. Also, see Table 5.1 for casting information details for the fabrication of the central parts and outer parts of 7LC assembly.

To eliminate the problem of the particles being on the surface of internal holes of the central part, some attempts to use platinum instead of plain carbon steel rods were made, but without success. For these attempts with platinum, dry ice covered the resultant central part, lowering the temperature to -40 °C to -70 °C at the platinum rods (attempting to use thermal contraction of the platinum in order to reduce the diameter of these rods). Apparently, the contraction of these

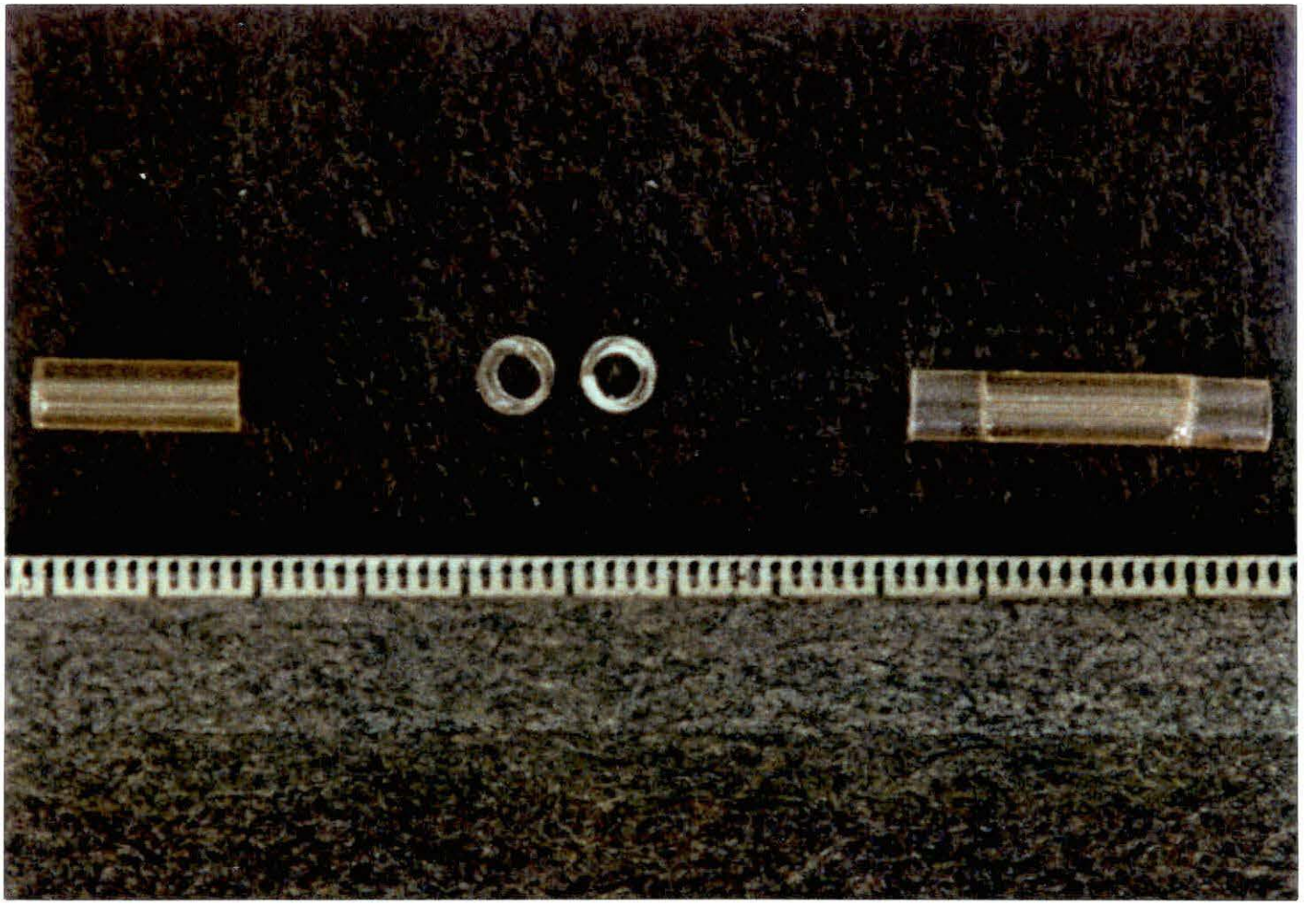

Figure 5.1: Views (from left to right) of the central part, outer parts, and D,L-PLA 7-lumen cuff. Scale bar = 1 mm (smallest intervals)

platinum (Pt) rods was not sufficient to permit the easy pull out of these rods from the central part. These Pt rods were broken in the pulling out attempt.

The weight and dimensions for the central parts ranged from 0.0976 to 0.1061 g for the weight, 9.6 to 10.52 mm for the length, 3.33 to 3.35 mm for the outer diameter, and 0.33 mm ID for the internal holes. The calculated density for these parts was 1.241 ± .018 g/cm^3. The weight and dimensions for the outer parts ranged from 0.0178 to 0.0186 g for the weight, 0.46 to 0.58 mm for

Table 5.1: Casting information for the fabrication of the central and outer parts of the 7LC

Sample	Duration of the melting process (hr)	Average rate of cooling** to room temperature (°C/min)		Cooling medium
		First 2 minutes	From 2 to 10 minutes	
Central part #1	4	65	4	Air
Central part #2	4	65	4	Air
Outer part #1*	4	65	4	Air
Outer part #2a	4	65	4	Air
Outer part #2b	4	65	4	Air

*Cut in two outer parts or projecting ends (1a and 1b) of the 7LC
**Thermocouple in contact with glass of the mold near the PLA

the wall thickness, 3.35 to 3.50 mm for the outer diameter, and 3.05 to 3.73 mm for the length. The length dimensions of the central and outer parts were similar to the proposed 7LC assembly dimensions (10 mm for the central part and 2 to 4 mm for the outer parts). There were no reported densities for the D,L-PLA cuff materials described in the literature, and so no comparisons can be made for this parameter. See Table 5.2 for the weight and dimensions for the central and outer parts fabricated for the 7LC assembly.

Table 5.2: Weight and dimensions for the central and outer parts of the 7LC assembly

Sample	Weight (g)	Length (mm)	Outside diameter (mm)	Inside diameter (mm)	Diameter of the internal holes (mm)
Central part #1	0.0976	9.60	3.33	NA*	0.33
Central part #2	0.1061	10.52	3.35	NA*	0.33
Outer part #1a	0.0184	3.63	3.35	2.45	NA*
Outer part #1b	0.0184	3.73	3.35	2.45	NA*
Outer part #2a	0.0178	3.05	3.50	2.34	NA*
Outer part #2b	0.0186	3.05	3.50	2.34	NA*

*NA = not applicable

5.2 Discussion

It was shown that it was feasible to make the D,L-PLA 7-lumen cuff without the use of high pressure or complex equipment. Of particular interest in the procedure was that sometimes microbubbles were formed after the melting process was complete, but before cooling the mold was complete (specifically at the bottom of the mold). This may be due to the elevated temperature (195-205 °C) and the lack of complete sealing at the union between the outer silicone rubber tubing and the modified 7-lumen tubing (original seven-lumen tubing from Daniel, 1991). Normally, these microbubbles disappeared after the mold cooled. Another problem that was seen in the fabrication of these cuffs was the presence of particles (maybe silicone rubber or plain carbon steel residues) in the surface of the internal holes of the central part of the lumen cuff. These residues were mostly removed by subsequent cleaning. Also, there was difficulty in aligning the 7-holes evenly with the silicone cap (modified 7-lumen tubing; see mold setup section and Figure 4.4) at the top of the mold pins. In the future, this difficulty can be resolved by inserting a modified capillary (similar to the one used to make the outer parts, but without sealing it; see mold setup section and Figure 4.3) to help in orienting and aligning the mold pins. The cutting, trimming, and positioning of the central and outer parts of cuff has to be improved

in order to have a better alignment of these parts for the gluing process and to minimize the formation of microbubbles in the glued region.

This is the first attempt to make a biodegradable multiple-lumen cuff. Only an indirect comparison with other fabrication results for biodegradable single lumen nerve guides (specifically, with PLA) can be made (Nyilas et al., 1983; Seckel et al., 1984). Many researchers have made tubular prostheses (single-lumen) of D,L-PLA using a dip-molding technique (Madison et al., 1984; Da Silva et al., 1985; Henry et al., 1985). For the fabrication of the multiple-lumen cuff, this dip-molding technique (a less tedious technique [especially with respect to the cleaning of the internal holes]) could be difficult to adapt. This can be difficult because seven PLA single lumen tubes would have to be done by this technique and then glued together (longitudinally). Then, the holes between the tubes would have to be filled with dissolved PLA material. This last step would be difficult to do because probably some bubbles would form between these tubes and also some misalignment between these tubes would be produced (due to the probability of dissolution of the tube walls by the solvent). Also, some initial attempts (not described) were made using a solvent centrifugal casting technique to make PLA plugs. These attempts did not work well because the plugs that were obtained were very porous (even when the PLA sam-

ples [in solution] stayed 12, 18, and 24 hours in the centrifuge at a maximum rotation speed of 3,000 rpm).

6. CONCLUSIONS

Most of the objectives of this work were realized. A biodegradable and biocompatible (D,L-PLA) nerve regeneration cuff (7-lumen) was successfully fabricated. The design and dimensions chosen for this biodegradable nerve cuff were selected to permit study of nerve regeneration in the sciatic nerves of rats, but they could be modified for larger nerves. Attempts to make an integral multiple lumen PLA (with the projecting ends and central part melted and joined at one time) did not work (not described). With larger mold systems, integral multiple lumen cuffs may be fabricated (with the use of negative molds of the projecting ends inserted on both ends [at the upper end and at the beginning of the naked pins inside the glass tube]). In this proposed mold setting, the flow of the melted material would be easier due to a lower physical impediment or larger space between the negative molds of the projecting ends inserted on both ends of the naked pins and the outer silicone rubber tubing (SR #1) (see Figure 4.4). The drawbacks of the cuff that was successfully fabricated are that it is not flexible and holes may have to be drilled on the projecting ends to permit suturing to a transected nerve. Also, the tedious cleaning that is necessary to remove the particles from the cuff internal holes is another drawback. Therefore, the mold system

described in this work has to be improved to avoid the deposition of particles on the interior lumenal surfaces of the 7LC and the subsequent cleaning. One way to do that could be by using Teflon pins instead of these silicone rubber covered steel pins. These Teflon pins could allow an easier pull out of the pins from the cuff without deposition of particles.

The D,L-PLA material is available commercially. This was the material used because it is less brittle than the L-PLA and the time for complete biodegradation is significatively lower for the same M_n (in six months,. D,L-PLA [M_n = 14,000)] biodegrades completely (Pitt et al., 1981) versus L-PLA [M_n =5,200] that biodegrades (weight loss) of 10% over a six month implantation period (Gogolewski et al., 1993)). The number average molecular weight of this D,L-PLA polymer was probably 13,400 and the M_w indicated by the supplier was approximately 20,000 (Engelberg, I. and J. Kohn. 1991). It should degrade completely in 28 weeks (this degradation period is recommended in the use of biodegradable implants because of their being less of a probability of inducing carcinogenesis (independent of the material used) [Gilding, 1981]) with a 5% and 25% of the mass loss at 4 and 12 weeks (Pitt et al., 1991). Many of the works with PLA single lumen nerve regeneration cuffs have used D,L-PLA material with M_w ranging from probably 20,000 (Nyilas et al., 1983) to 100,000 (Seckel et al., 1984). In these studies, the mechanical integrity of this D,L-PLA

single lumen cuff appeared to be maintained at least for 3 to six weeks (Nyilas et al., 1983), and that is approximately when nerve regeneration takes place across a nerve gap of 10 mm in rat transected nerves (Williams et al., 1983). Then, it is anticipated that these cuffs could be used initially in animal studies (for example, rats) because nerve regeneration across these cuffs could be successful (a 10 mm nerve gap may be bridged from 3 to 4 weeks with a formation of myelinated axons and a perineurial-like sheet [Williams et al., 1983]). Such *in vivo* preliminary studies can now be performed for the biodegradable 7LC.

Future work, in addition to that mentioned, would be the fabrication (and use on animals) of biodegradable 7-lumen cuffs with D,L-PLA of higher number average molecular weight (M_n), for example with 49,000 and 100,000, that would initiate mass loss after 20 or 34 weeks of implantation, respectively. Also, they would be completely degraded by one year (M_n = 49,000) or by 18 months (M_n = 100,000). By utilizing a multiple lumen PLA cuff, the likelihood of successful regeneration of nerves is high and these cuffs may offer results superior to those seen using experimental single lumen PLA cuffs.

BIBLIOGRAPHY

Daniel, J. M. K. 1991. Reorganization and orientation of peripheral nerve fibers regenerating through a multiple-lumen silicone rubber cuff: An experimental study using the sciatic nerve of rats. Ph. D. Dissertation. Iowa State University. 152 pages.

Daniel, R. K. and J. K. Terzis. 1977. Structure and function of the peripheral nerve. Page 295-319 in R. K. Daniel and J. K. Terzis, eds. *Reconstructive Microsurgery*. Little, Brown and Company, Boston.

Da Silva, C. F., R. Madison, P. Dikkes, T. H. Chiu, and R. L. Sidman. 1985. An *in vivo* model to quantify motor and sensory peripheral nerve regeneration using bioresorbable nerve guides tubes. *Brain Res.* 342: 307-315.

Dellon, A. L and Mackinnon S. E. 1988. An alternative to the classical nerve graft for the management of the short nerve gap. *Plastic and Reconstructive Surgery* 82: 849-856.

Den Dunnen, W. F. A., B. van der Lei, J. M. Schakenraad, E. H. Blaauw, I. Stokroos, A. J. Pennings, and P. H. Robinson. 1993. Long-term evaluation of nerve regeneration in a biodegradable nerve guide. *Microsurgery* 14: 508-515.

Dijkstra, P. J., M. J. D. Eenink, and J. Feijen. 1990. Alpha-hydroxy acid based biodegradable polymers poly(L-lactide) and polydepsipeptides. Pages 99-142 in S. A. Barenberg, J. L. Brash, R. Narayan, and A. E. Redpath, eds. *Degradable Materials: Perspective, Issues, and Opportunities.* CRC Press, Boca Raton, Florida.

Engelberg, I. and J. Kohn. 1991. Physico-mechanical properties of degradable polymers used in medical applications: A comparative study. *Biomaterials* 12: 292-304.

Gilding, D. K. 1981. Biodegradable polymers. Pages 209-232 in D. F. Williams, ed. *Biocompatibility of Clinical Implant Materials Volume II.* CRC Press, Boca Raton, Florida.

Gilding, D. K. and A. M. Reed. 1979. Biodegradable polymers for use in surgery-polyglycolic/poly(actic acid) homo- and copolymers: 1. *Polymer* 20: 1459-1464.

Gogolewski, S., M. Jovanovic, S. M. Perren, J. G. Dillon, and M. K. Hughes. 1993. Tissue response and in vivo degradation of selected polyhydroxyacids: Polylactides (PLA), poly(3-hydroxybutyrate) (PHB), and poly(3-hydroxybutyrate-co-3-hydroxyvalerate) (PHB/VA). *Journal of Biomedical Materials Research* 27: 1135-1148.

Guénard, V., R. F. Valentini, and P. Aebischer. 1991. Influence of surface texture of polymeric sheets on peripheral nerve regeneration in a two-compartment guidance system. *Biomaterials* 12: 259-263.

Hanson, S. M. and M. E. McGinnis. 1994. Regeneration of rat sciatic nerves in silicone tubes: Characterization of the response to low intensity d.c. stimulation. *Neuroscience* 58: 411-421.

Henry, E. W., T. H. Chiu, E. Nyilas, T. M. Brushart, P. Dikkes, and R. L. Sidman. (1985). Nerve regeneration through biodegradable polyester tubes. *Exp. Neuro.* 90: 652-676.

Hentz, V. R., J. M. Rosen, S. J. Xiao, K. C. McGill, and G. Abraham. 1991. A comparison of suture and tubulization nerve repair techniques in a primate. *J. of Hand Surgery* 16 A: 251-261.

Hoppen, H. J., J. W. Leenslag, A. J. Pennings, B. van der Lei, and P. H. Robinson. 1990. Two-ply biodegradable nerve guide: basic aspects of design, construction and biological performance. *Biomaterials* 11: 286-290.

Junqueira, L. C. and J. Carneiro. 1980. Nerve tissue. Pages 152-185 in L. C. Junqueira and J. Carneiro, eds. *Basic Histology*. Lange Medical Publications, Los Altos, California.

Keeley, R. D., K. D. Nguyen, M. J. Stephanides, J. Padilla, J. M. Rosen. 1991. The artificial nerve graft: A comparison of blended elastomer-hydrogel with polyglycolic acid conduits. *J. of Reconstructive Microsurgery* 7: 93-100.

Knoops, B., H. Hurtado, and P. van den Bosch de Aguilar. 1990. Rat sciatic nerve regeneration within an acrylic semipermeable tube and comparison with a silicone impermeable material. *J. Neuropathol. and Exp. Neurol.* 49: 438-448.

Kronenthal, R. L. 1975. Biodegradable polymers in medicine and surgery. Pages 119-137 in R. L. Kronenthal, Z. Oser, and E. Martin, eds. *Polymers in Medicine and Surgery*. Plenum Press, New York.

Kumar, G. S. 1987. Biodegradation of Synthetic Polymers: An Overview. Pages 25-76 in Kumar, ed. *Biodegradable Polymers: Prospects and Progress.* Marcel Dekker, Inc. New York, New York.

Mackinnon, S. E. and A. L. Dellon. 1990. Clinical nerve reconstruction with a bioresorbable polyglycolic acid tube. *Plastic and Reconstructive Surgery* 85: 419-424.

Madison, R., C. da Silva, P, Dikkes, T. H. Chiu, and. R. L. Sidman. 1985. Increased rate of peripheral nerve regeneration using bioresorbable nerve guides and a laminin-containing gel. *Exp. Neuro.* 88: 767-772.

Madison, R., C. da Silva, P. Dikkes, R. L. Sidman, and T. H. Chiu. 1987. Peripheral nerve regeneration with entubulization repair: Comparison of biodegradable nerve guides versus polyethylene tubes and the effects of a laminin-containing gel. *Exp. Neuro.* 95: 378-390.

Madison, R., R. L. Sidman, E. Nyilas, T. H. Chiu, and D. Greatorex. 1984. Nontoxic nerve guide tubes support neovascular growth in transected rat optic nerve. *Exp. Neuro.* 86: 448-461.

Maeda, T., S. E. Mackinnon, T. J. Best, P. J. Evans, D. A. Hunter, and R. T. Rajiv Midha. 1993. Regeneration across 'stepping-stone' nerve grafts. *Brain Res.* 618: 196-202.

Marshall, D. M., M. Grosser, M. C. Stephanides, R. D. Keeley, and J. M. Rosen. 1989. Sutureless nerve repair at the fascicular level using a nerve coupler. *J. of Rehabilitation Research and Development* 26: 63-76.

Martini, F. 1989. The nervous system: Neural tissue. Page 308-335 in F. Martini, ed. *Fundamentals of Anatomy and Physiology.* Prentice-Hall, Englewood Cliffs, New Jersey.

Molander H., O. Engkvist, J. Hagglund, Y. Olsson, and E. Torebjork. 1983. Nerve repair using a polyglactin tube and nerve graft: An experimental study in the rabbit. *Biomaterials* 4: 276-280.

Molander H., Y. Olsson, O. Engkvist, S. Bowald, and I. Eriksson. 1982. Regeneration of peripheral nerve through a polyglactin tube. *Muscle & Nerve* 5: 54-57.

Nyilas E., T. H. Chiu, R. L. Sidman, E. W. Henry, T. M. Brushart, P. Dikkes, and R. Madison. 1983. Peripheral nerve repair with bioresorbable prosthesis. *Trans. Am. Soc. Artif. Intern Organs* 29: 307-312.

Pham, H. N., J. A. Padilla, K. D. Nguyen, and J. M. Rosen. 1991. Comparison of nerve repair techniques: Suture vs. avitene-polyglycolic acid tube. *J. of Reconstructive Microsurgery* 7: 31-36.

Pistner, H., D. R. Bendix, J. Mühling, and J. F. Reuther. 1993 a. Poly(L-lactide): a long term degradation study in vivo [Part III. Analytical characterization]. *Biomaterials* 14: 291-298.

Pistner, H., R. Gutwald, R. Ordung, and J. Reuther. 1993 b. Poly(L-lactide): a long term degradation study in vivo [I. Biological results]. *Biomaterials* 14: 671-677.

Pitt, C. G., M. M. Gratzl, G. L. Kimmel, J. Surles, and A. Schindler. 1981. Aliphatic polyesters II. The degradation of poly (DL-lactide), poly (ε-caprolactone), and their copolymers in vivo. *Biomaterials* 2: 215-220.

Reid, R. L., D. E. Cutright, and J. S. Garrison. 1978. Biodegradable cuff an adjunct to peripheral nerve repair: A study in dogs. *The Hand.* 10: 259-266.

Rosen, J. M., V. R. Hentz, and E. N, Kaplan. 1983. Fascicular tubulization: A cellular approach to peripheral nerve repair. *Annals of Plastic Surgery* 11: 397-411.

Rosen, J. M., J. A. Padilla, K. D. Nguyen, M. A. Padilla, E. E. Sabelman, and H. N. Pham. 1990. Artificial nerve graft using collagen as an extracellular matrix for nerve repair compared with sutured autograft in a rat model. *Annals of Plastic Surgery* 25: 375-387.

Rosen, J. M., J. A. Padilla, K. D. Nguyen, J. Siedman and H. N. Pham. 1992. Artificial nerve graft using glycolide trimethylene carbonate as a nerve conduit filled with collagen compared to sutured autograft in a rat model. *J. of Rehabilitation Research and Development.* 29: 1-12.

Rosen, J. M., H. N. Pham, G. Abraham, and L. Harold. 1989. Artificial nerve graft compared to sutured autograft in a rat model. *J. of Rehabilitation Research and Development.* 26: 1-14.

Satou, T., S. Nishida, S. Hiruma, K. Tanji, M. Takahashi, S. Fujita, Y. Mizuhara, F. Akai, and S. Hashimoto. 1986. A morphological study on the effects of collagen gel matrix on regeneration of severed rat sciatic nerve in silicone tubes. *Acta Pathol. Jpn.* 36: 199-208.

Schindler, A., R. Jeffcoat, G. L. Kimmel, C. G. Pitt, M. E. Wall, and R. Zweidinger. 1977. Biodegradable polymers for sustained drug delivery. Page 251-

289 in E. M. Pearce and J. R. Schaefgen, eds. *Contemporary Topics in Polymer Science.* Plenum Press, New York, New York.

Seckel, B. R., T. H. Chiu, E. Nyilas, and R. L. Sidman. 1984. Nerve regeneration through synthetic biodegradable nerve guides: Regulation by the target organ. *Plastic and Reconstructive Surgery* 74: 173-181.

Spencer, P. S. 1977. Morphology of the injured nerve. Page 342-349 in R. K. Daniel and J. K. Terzis, eds. *Reconstructive Microsurgery.* Little, Brown and Company, Boston, Mass.

Swaim, S. F. 1987. Peripheral nerve surgery. Pages 493-498 in J. E. Oliver, B. F. Hoerlein, and I. G. Mayhew, eds. *Veterinary Neurology.* W. B. Saunders Company, Philadelphia, PA.

Therin, M., P. Christel S. Li, H. Garreau, and M. Vert. 1992. *In vivo* degradation of massive poly[α-hydroxy acids]: validation of *in vitro* findings. *Biomaterials* 13: 594-600.

Vert, M. 1990. Degradation of polymeric biomaterials with respect to temporary therapeutic applications: Tricks and treats. Pages 11-37 in S. A. Barenberg, J. L. Brash, R. Narayan, and A. E. Redpath, eds. *Degradable Materials: Perspective, Issues, and Opportunities.* CRC Press, Boca Raton, Florida.

Williams, D. F. 1989. A model for biocompatibility and its evaluation. *J. Biomed. Eng.* 11: 185-191.

Williams, L. R., N. Danielsen, H. Muller, and S. Varon. 1987. Exogenous matrix precursors promote functional nerve regeneration across a 15-mm gap within a silicone chamber in the rat. *J. of Comparative Neurology* 264: 284-290.

Williams, L. R., F. M. Longo, H. C. Powell, G. Lundborg, and S. Varon. 1983. Spatial-temporal progress of peripheral nerve regeneration within a silicone chamber: Parameters for a bioassay. *J. of Comparative Neurology* 218: 460-470.

Zellem, R. T., D. W. Miller, J. A. Kenning, E. M. Hoenig, and W. A. Buchheit. 1989. Experimental peripheral nerve repair: Environmental control directed at the cellular level. *Microsurgery* 10: 290-301.

ACKNOWLEDGMENTS

I thank my major professor, Dr. Raymond T. Greer, for his support and direction during this research. Also, I thank to Dr. Mary Helen Greer and Dr. David Merkley for agreeing to serve as members of my committee. I also thank my fellow students and other members of the Biomedical Engineering Program for their ideas and cooperation.

Especially, I give my thanks to God, our Lord, for his mercy and care on my family and me throughout this endeavor. I also especially thank my wife for her encouragement, great patience, and love throughout my studies. Finally, I thank my children for the great joy and love that I receive from them.

APPENDIX: LIST OF ACRONYMS

Acronyms	Complete Name
ANG	artificial nerve graft
DRG	dorsal root ganglia cell bodies
DS	double stepping-stone nerve graft
FE	fracture elongation
FSM	flexural storage modulus or bending modulus of elasticity
GTMC	glycolide trimethyl carbonate
HEB	hydrogel-elastomer biopolymer
HLA/S	copoly [1,6-hexylene-(1,1)-L-lactate/succinate]
HRP	horseradish peroxidase
ID	inside diameter
ln	natural logarithm
MA	myelinated axons
MLC	multiple-lumen cuff
M_n	number average molecular weight
MP_a	megapascal[a]
MW	molecular weight
M_w	weight average molecular weight
OD	outside diameter
PBS	poly(2,3-butylene succinate)
PCL	poly-ε-caprolactone
PE	polyethylene
PGA	polyglycolic acid
PGL	polyglactin
PLA	polylactic acid
SAG	suture autograft nerve
SLC	single-lumen cuff
SR	silicone rubber
T_d	dissociation temperature
TEC	triethyl citrate
T_g	glass transition temperature
T_m	melting point
TM	tensile modulus
TS	tensile strength
VH	ventral horn cell bodies
WT	wall thickness
7LC	seven lumen cuff

[a] 1 megapascal = 145 pounds per square inch